



**HAL**  
open science

# Probability of detection and positioning error of a hydro acoustic telemetry system in a fast-flowing river: Intrinsic and environmental determinants

J. Bergé, Hervé Capra, H. Pella, T. Steig, M. Ovidio, E. Bultel, Nicolas  
Lamouroux

## ► To cite this version:

J. Bergé, Hervé Capra, H. Pella, T. Steig, M. Ovidio, et al.. Probability of detection and positioning error of a hydro acoustic telemetry system in a fast-flowing river: Intrinsic and environmental determinants. *Fisheries Research*, 2012, 125-126, p. 1 - p. 13. 10.1016/j.fishres.2012.02.008 . hal-00704901

**HAL Id: hal-00704901**

**<https://hal.science/hal-00704901>**

Submitted on 6 Jun 2012

**HAL** is a multi-disciplinary open access archive for the deposit and dissemination of scientific research documents, whether they are published or not. The documents may come from teaching and research institutions in France or abroad, or from public or private research centers.

L'archive ouverte pluridisciplinaire **HAL**, est destinée au dépôt et à la diffusion de documents scientifiques de niveau recherche, publiés ou non, émanant des établissements d'enseignement et de recherche français ou étrangers, des laboratoires publics ou privés.

1 **Probability of detection and positioning error of a hydro acoustic telemetry**  
2 **system in a fast-flowing river: intrinsic and environmental determinants**

3  
4  
5

6 Julien Bergé <sup>a,\*</sup>, Hervé Capra <sup>a</sup>, Hervé Pella <sup>a</sup>, Tracey Steig <sup>b</sup>, Michaël Ovidio <sup>c</sup>, Elise Bultel <sup>a</sup>,  
7 N. Lamouroux <sup>a</sup>.

8  
9  
10

11 <sup>a</sup> IRSTEA, UR MALY, Laboratory Dynam, 3 bis Quai Chauveau - CP 220, F-69336 LYON,  
12 France.

13 <sup>b</sup> Hydroacoustic Technology Inc., 715 NE Northlake Way, Seattle, WA 98105, USA.

14 <sup>c</sup> University of Liège, Biology of Behaviour Unit-Cefra, Laboratory of Fish Demography and  
15 Hydroecology (LDPH), 10 Chemin de la Justice, 4500 Tihange, Belgium.

16  
17  
18

19 \*Corresponding author: Hervé Capra. Tel.; +334 7220 8732; fax: +334 7847 7875

20  
21  
22  
23  
24  
25

E-mail addresses: [julien.berge@irstea.fr](mailto:julien.berge@irstea.fr) (J. Bergé), [herve.capra@irstea.fr](mailto:herve.capra@irstea.fr) (H. Capra),  
[herve.pella@irstea.fr](mailto:herve.pella@irstea.fr) (H. Pella), [tsteig@htisonar.com](mailto:tsteig@htisonar.com) (T. Steig), [M.Ovidio@ulg.ac.be](mailto:M.Ovidio@ulg.ac.be) (M.  
Ovidio), [elise.bultel@gmail.com](mailto:elise.bultel@gmail.com) (E. Bultel), [Nicolas.lamouroux@irstea.fr](mailto:Nicolas.lamouroux@irstea.fr) (N. Lamouroux).

26     ***Abstract***

27

28     *In situ* fixed acoustic telemetry methods make it possible to study simultaneously the  
29 detailed movements of individual fish and their relationship to the environment, but the  
30 properties of these methods is little known in harsh physical conditions. We examined the  
31 probability of tag detection by the system and the positioning error for detected tags of an  
32 existing telemetry system installed with 32 fixed hydrophones in a reach of the fast-flowing  
33 Rhône River in France. The reach was 1.8 km long and had heterogeneous thermal and  
34 hydraulic conditions described by a two-dimensional hydraulic model. We compared  
35 positions detected by the system with true positions estimated using a tachometer or a  
36 differential GPS, for various sets of experimental tag emissions. We analyzed how the  
37 probability of detection and the positioning error were affected by user-defined variables and  
38 three groups of environmental variables describing the configuration of the hydrophones  
39 around tag position, the physical environment at tag position and the reception quality. Tag  
40 emissions from the center channel had an average probability of detection (40-50%) higher  
41 than emissions originating from positions close to the banks, and were positioned with smaller  
42 average errors (3-5m). The probability of detection of emissions typically varied between near  
43 0% and 80% with configuration variables (density of surrounding hydrophones and location  
44 of tag relative to the hydrophones) and also decreased in the presence of coarse substrate. The  
45 positioning error was mainly reduced when user-defined variables of the triangulation  
46 software were set by an expert user. Configuration variables also influenced the positioning  
47 error with weaker effects than those observed for detection probability.

48

49     **1. Introduction**

50

51 The sensitivity of fish and other freshwater organisms to changes in abiotic conditions of  
52 rivers has been reported in many studies with a particular emphasis on their ecological (e.g.,  
53 behavioral, demographic, physiological) responses to modifications of hydrological or  
54 thermal regimes (Minns et al., 1996; Lukšienė et al., 2000; Vehanen et al., 2000; Ovidio et al.,  
55 2008; Craven et al., 2010; Olden and Naiman, 2010; Poff and Zimmerman, 2010). In  
56 particular, individual fish movements have often been related to short-term changes in  
57 discharge rate and temperature (Ovidio et al., 1998; Ovidio and Philippart, 2008). Behavioral  
58 studies in aquatic systems increasingly use biotelemetry (Lyons and Lucas, 2002; Cooke et  
59 al., 2004; Geeraerts et al., 2007; Ovidio et al., 2007) to record individual fish movements at  
60 different time steps, from seconds to multiple years (Lucas and Batley, 1996; Meyer and  
61 Hinrichs, 2000; Ehrenberg and Steig, 2003). The probability of detection and the positioning  
62 error are major characteristics of telemetry systems and have been improved in recent years.  
63 Low errors are essentially obtained with fixed acoustic telemetry systems that provide detailed  
64 information when sound transmitters (i.e. tags) are detected by acoustic hydrophones  
65 (Ehrenberg and Steig, 2003; Cooke et al., 2005). Compared to other systems, fixed systems  
66 enable the simultaneous detailed study of the movements of many individual fish. However, a  
67 better quantification of their properties is needed to find appropriate compromises between the  
68 probability of detection, the positioning error and the surface area covered by the system. For  
69 example, Clements et al. (2005) showed that the probability of detection of the VR2 system  
70 (Vemco Ltd, Canada) could vary between 0 and 100% in a stream reservoir and an estuary  
71 depending on the placement of the hydrophones and their mooring method. Cote et al. (1998),  
72 using the MAP\_500 Lotek<sup>®</sup> system (Lotek Marine Technologies Inc., Ca) in the Bonavista  
73 Bay (Newfoundland, Canada), reported an average positioning error of 2 m or less inside the  
74 baseline of hydrophones used during a two months tracking of juvenile Atlantic cods (*Gadus*  
75 *morhua*, pulse rate of 5 min). The 3-dimensionnal positioning error of the Vemco radio-

76 acoustic positioning system was estimated in a South African bay (O'dor et al., 1998) to be  
77 about 1-2 m inside the hydrophones array and about 3-5 meters when emissions were 100 m  
78 outside the array.

79  
80 The probability of detection and the positioning error of telemetry systems potentially  
81 depend on a large number of intrinsic and environmental factors (Kell et al., 1994; Voegeli  
82 and Pincock, 1996). Intrinsic factors include the estimation of the speed of sound, the  
83 knowledge of exact hydrophone positions and the adjustment of the parameters of the  
84 positioning software (Juell and Westerberg, 1993; Cote et al., 1998; Wahlberg et al., 2001;  
85 Ehrenberg and Steig, 2002). Among environmental factors, weak spatial configurations of  
86 hydrophones relative to the tag location (long distances, narrow viewing angles) have been  
87 identified as influencing the probability of detection and the positioning error (Baras and  
88 Lagardère, 1995; Smith et al., 1998; Ehrenberg and Steig, 2002; Niezgoda et al., 2002;  
89 Simpfendorfer et al., 2002; Heupel et al., 2006; Espinoza et al., 2011). In addition, the  
90 probability of detection and the positioning error likely decrease in heterogeneous substrate,  
91 hydraulic and thermal conditions that can favor sound refraction, ambient noise and variations  
92 in speed of sound (Voegeli and Pincock, 1996; Trevorrow, 1998; Ehrenberg and Steig, 2002).  
93 Quantifying the combined influence of intrinsic and environmental characteristics of the study  
94 site on the system properties can improve further study designs. It is particularly needed for  
95 telemetric studies made in fast-flowing rivers, whose heterogeneous physical characteristics  
96 may complicate tag detection and positioning.

97  
98 In summer 2009, an acoustic fixed telemetry system (HTI<sup>®</sup>) was installed in a physically  
99 heterogeneous reach of the fast-flowing Rhône River in France to analyze the behavioral  
100 response of fish to variations in discharge rate (due to hydropeaking) and water temperature

101 (warm water is discharged in the reach by a nuclear power plant). In this paper, we describe  
102 how we used this installation (1) to quantify the probability of detection and the positioning  
103 error of the telemetry system in a fast-flowing heterogeneous river, (2) to infer which intrinsic  
104 and environmental variables influence the detection and the position errors, and (3) to discuss  
105 methods for optimizing installations in future studies. For this purpose, we simultaneously  
106 estimated tag positions in the river using the HTI<sup>®</sup> system and using an independent  
107 "reference" differential GPS or tachometer. We studied how the probability of detection and  
108 the positioning error were affected by the user-defined variables in the telemetry system  
109 (intrinsic variables), and various environmental variables associated with tag positions.

110

## 111 **2. Materials and methods**

112

### 113 *2.1. Study Site*

114

115 The Rhône river has a drainage basin area of 98,556 km<sup>2</sup> and a mean annual discharge of  
116 1,720 m<sup>3</sup>.s<sup>-1</sup> at its mouth (Olivier et al., 2009). Our study reach was 1.8 km long and 140 m  
117 wide (at mean discharge) and was situated at Bugey (45° 47'N; 5°16' E), upstream from the  
118 confluence of the Ain River and the town of Lyon, in the longest Rhône segment without  
119 discharge derivation (Fig. 1). The Rhône at Bugey has a nival hydrological regime (i.e. under  
120 the influence of snowmelt) characterized by a mean monthly discharge ranging from 387 m<sup>3</sup>.s<sup>-1</sup>  
121 <sup>1</sup> in September to 567 m<sup>3</sup>.s<sup>-1</sup> in June. Mean annual discharge is 473 m<sup>3</sup>.s<sup>-1</sup>, and the mean daily  
122 discharge ranges from 197 m<sup>3</sup>.s<sup>-1</sup> (exceeded 95 % of the time) to 933 m<sup>3</sup>.s<sup>-1</sup> (exceeded 5 % of  
123 the time). A high discharge variability (daily changes up to 700 m<sup>3</sup>.s<sup>-1</sup>, Olivier et al., 2009) is  
124 generally observed during the week due to hydropeaking at upstream dams, and discharge is  
125 generally lower and more stable during week-ends. At mean discharge, point depth-averaged

126 velocity reaches  $1.8 \text{ m}\cdot\text{s}^{-1}$  and point depth reaches 8 m. The substrate composition was  
127 mapped using a combination of visual observations from a boat and high resolution aerial  
128 photographs. Substrate size was assigned to one of five ordinal classes and consisted of  
129 pebbles (36.0 % of the surface area), gravel (26.4 %), stones (14.4 %), blocks (13.9 %) and  
130 sand (8.2 %). The daily water temperature upstream from the study reach ranged in 2009 from  
131  $2.8 \text{ }^{\circ}\text{C}$  to  $23.6 \text{ }^{\circ}\text{C}$  (Roger et al., 2010). A nuclear power plant (Bugey Power Plant), located on  
132 the west bank of the study reach, extracts  $100 \text{ m}^3\cdot\text{s}^{-1}$  to cool reactors and discharges warmer  
133 water (between 8 and  $10 \text{ }^{\circ}\text{C}$  warmer) at two different places (Fig. 1), creating a strong  
134 transversal thermal heterogeneity. No vertical thermal stratification was observed in the reach  
135 (Capra et al., 2008). Downstream from the nuclear power plant, the warmed water cools down  
136 by around  $1 \text{ }^{\circ}\text{C}$  per kilometer, and diffuses from the west bank to the whole channel 10 km  
137 downstream (Capra et al., 2008). Water turbidity recorded in 2009 ranged between  $9.5 \text{ mg}\cdot\text{l}^{-1}$   
138 in February and  $81 \text{ mg}\cdot\text{l}^{-1}$  in November (Roger et al., 2010).

139  
140 A two-dimensional hydraulic model of the reach was developed using (1) a digital  
141 elevation model based on extensive field measurements of topography and bathymetry (an  
142 average of four measuring points per  $\text{m}^2$ , Pella et al., 2007), (2) water level - discharge  
143 relationship records, and (3) velocity measurements at different discharge rates (Capra et al.,  
144 2011). The hydraulic model was calibrated and validated for a discharge rate between 150 and  
145  $850 \text{ m}^3\cdot\text{s}^{-1}$ . Differences between simulated and measured water levels were found to be around  
146 1 cm, and a comparison of measured and simulated velocities did not show errors exceeding  
147  $0.1 \text{ m}\cdot\text{s}^{-1}$  across the study site (Capra et al., 2011).

148

149 *2.2. Telemetry system principles and deployment*

150

151 We used an HTI<sup>®</sup> automatic acoustic telemetry system that included a set of pre-positioned  
152 hydrophones used to detect ultrasounds emitted by acoustic tags of various sizes, programmed  
153 with a frequency of 307 KHz (Ehrenberg and Steig, 2003). Each hydrophone was cabled to a  
154 receiver unit (the Acoustic Tag Receiver, model 290) that recorded acoustic signals and stored  
155 them on a computer. The Acoustic Tag Receiver was synchronized with UTC time (Universal  
156 Time Coordinated) thanks to an internal GPS, and its digital signal processor had a precision  
157 of 12 KHz. We used Model 795G tags (transmit power level: 155 dB relative to 1  $\mu$ Pa at 1 m;  
158 length: 25 mm; diameter: 11 mm; weight: 3.1 g). The average lifetime of tags was about 50  
159 days in our experimental conditions (according to the manufacturer). Tag signals were series  
160 of pulses (1 ms long in our experiment) sent with different periods P (P varied around 3s in  
161 our experiment) that were used to identify and track individual tags. A secondary signal,  
162 called “subcode”, which was a replication of the first signal, was used to improve tag signal  
163 reception and the identification of each tag in noisy environments. The subcode was usually  
164 not used for positioning tags, but sometimes it could be considered by the system as another  
165 principal signal. In such a case, two positions were estimated with close emission times. Such  
166 “duplicate” positions were identified and filtered. In our experiment, we positioned tags in  
167 two dimensions (2D). A three dimensional (3D) positioning of tags was not feasible because  
168 the study site had too little vertical separation in the hydrophone array to resolve tag depth.  
169 For our 2D analysis, the acoustic tag signal must be received by at least three hydrophones.  
170 Only three hydrophones were selected by the system to position a given tag and are called  
171 thereafter the “listening trio”. During a post treatment stage, arrival times of pulses received  
172 by hydrophones were used to estimate the coordinates of tags at signal emission and the  
173 emission time. The post treatment of the acoustic signals (filtering and triangulation) was  
174 made using successively two HTI<sup>®</sup> proprietary softwares (see <http://www.htisonar.com/>).  
175

176 A total of 32 hydrophones were installed in May 2009 (Fig. 1) and 16 km of weighted  
177 acoustic cables were used to connect them to the Acoustic Tag Receiver. The connection of  
178 acoustic cables to the hydrophones was made by a diver. Each hydrophone was mounted on a  
179 concrete block of 300 kg (Fig. 2) and deposited on the river bed using a boat; an operation  
180 that was sometimes difficult due to high current velocities. The hydrophone was positioned  
181 about 10 cm above the block, and the block could constitute an acoustic shadow for signals  
182 emitted from the bottom within an area of about 10 m<sup>2</sup> around the block. Hydrophone  
183 positions were pre-defined using the digital elevation model so that most emission points  
184 could be *a priori* heard by more than three hydrophones, as recommended by Kell et al.  
185 (1994) or Voegeli and Pincock (1996), while taking into account that the theoretical detection  
186 (hearing) range of hydrophones was 300 m (according to the manufacturer). We released  
187 hydrophones at pre-defined positions using a dGPS (Leica<sup>®</sup> 1200) and a real time track  
188 process on a computer taken on board. Pre-defined coordinates were stored in Matrix M1.  
189 Because of local hydraulic or substrate constraints, seven hydrophones were positioned a few  
190 meters away from their pre-defined position. Their theoretical coordinates in M1 were  
191 replaced by coordinates measured in the field with a tachometer (Leica<sup>®</sup> 800). At the end of  
192 the study (on September 18, 2009), the coordinates of the hydrophones were again measured  
193 with a dGPS (Leica<sup>®</sup> 1200) and were stored in Matrix M2.

194

### 195 2.3. Data used for estimating the probability of detection and positioning errors

196

197 Two different sets of data were collected, one by dragging tags over the whole study site  
198 from a boat (drags data), and the other by holding tags at fixed locations along the banks  
199 (banks data). In both cases, the objective was to compare tag positions estimated by the HTI<sup>®</sup>  
200 system with reference positions measured by dGPS or tachometer. We estimated the detection

201 probability of tags by the proportion of known emissions actually positioned by the HTI<sup>®</sup>  
202 system, and the positioning error of detected tags by the Euclidian distance between HTI<sup>®</sup>  
203 estimated position and the reference positions. The dGPS and tachometer systems used have  
204 themselves a centimetric positioning error (given in Takac and Walford, 2006, for the dGPS  
205 and by the manufacturer for the tachometer) and we assumed that they provided true  
206 positions. Because the errors of the dGPS and tachometer and the errors of the HTI<sup>®</sup> system  
207 can be assumed independent, our estimation of positioning error is conservative.

208  
209 Drags data were collected with the dGPS during two surveys of the whole site by boat (Fig.  
210 1), following zigzag trajectories at reduced relative velocity (less than  $1 \text{ m}\cdot\text{s}^{-1}$ ) to limit  
211 potential effects of the boat movement on the probability of detection (Melnychuk and  
212 Christensen, 2009). Characteristics of the two drag surveys are presented in Table 1. A  
213 NKE<sup>®</sup>- SP2T sonde ( $\pm 0.05^\circ\text{C}$ ) recorded water temperature every second. During drags, we  
214 used four tags with emission periods P equal to 3051, 3079, 3121 and 3247 ms, and subcodes  
215 emitted 225 ms after the principle signal. Tags were attached to the base of a pole supporting  
216 the antenna of the dGPS: two tags were submerged 50 cm below the surface and two tags  
217 were submerged at 1 m. UTC time was assigned to each boat's position recorded by the dGPS  
218 (frequency: 1 Hz). The data corresponding to the four tags were pooled for the analyses. The  
219 banks data set was less extensive and targeted shallower habitats where the boat could not  
220 navigate and where the dGPS could not work due to the presence of trees. We collected these  
221 data over two days (June 24-25, 2009) with a tachometer at 114 fixed locations chosen along  
222 both banks of the study site (Fig. 1). Characteristics of banks measurements are presented in  
223 Table 1. One tag (with P equal to 3121 or 3205 ms and subcode set up at 225 ms) was  
224 attached to the tachometer tip and we submerged the tag during a 15 seconds sequence just  
225 under the surface and just above the bed (one sequence each) at each fixed location. Each

226 fixed location was measured for each sequence of 15 seconds and a UTC time was recorded  
227 for each tachometer measurement.

228

#### 229 *2.4. Estimating true positions at emission times*

230

231 All periods of times with dGPS gaps (absence of data) longer than 5 seconds were removed  
232 from all analyses to reduce dGPS interpolation errors. Before analyzing detection probability  
233 and positioning errors, we estimated true positions at emission times (UTC) using the dGPS  
234 and tachometer data, for all emissions, detected or not, by the HTI<sup>®</sup> system. Concerning  
235 positions detected by the HTI<sup>®</sup> system, the dGPS positions of drag data corresponding to the  
236 emission times ( $t_i$ ) were interpolated from the raw dGPS data (gaps up to 5 s) using cubic  
237 spline functions that smoothed the x and y dGPS coordinates (Fritsch and Carlson, 1980; R  
238 Development Core Team 2010). Concerning positions undetected by the HTI<sup>®</sup> system, virtual  
239 emission times were estimated. Specifically, for each tag of emission period P and for each  
240 detected emission time by the HTI<sup>®</sup> system ( $t_i$ ), if no position was estimated at  $t_i + P$  (+/- 0.5  
241 second of tolerance), we considered that an emission was undetected. In this case, we  
242 considered that  $t_i + P$  was a virtual emission time. The virtual coordinates of this virtual  
243 emission time were interpolated from the dGPS data as described above and the position  
244 obtained was called a “virtual position”. Several (k) consecutive virtual emission times could  
245 be identified using the same principle, and these virtual emission times were set as  $t_i + P$ ,  $t_i +$   
246  $2P$  ...  $t_i + kP$ . Similarly, virtual emission times were identified between the start of the  
247 experiment and the first detection.

248

#### 249 *2.5. Intrinsic and environmental variables relationship with the probability of detection and* 250 *positioning errors*

251

252 We organized explanatory variables into one group of user-defined variables, and three  
253 groups of environmental variables: (1) the configuration of hydrophones surrounding tag  
254 positions (detected and virtual), (2) the physical characteristics at tag positions (detected and  
255 virtual), and (3) indicators of reception conditions (detected positions only). All variables  
256 were calculated similarly for drags and banks data.

257

258 User-defined variables can affect both detection probability and positioning error. These  
259 variables include: (1) the speed of sound (SpS), which determined how time was translated  
260 into distances in the positioning algorithm, (2) the hydrophone coordinates listed in the  
261 positions Matrix (M) and (3) a series of 19 Post-Treatment parameters (PT, detailed in  
262 Supplementary file S1). We analyzed the effects of SpS by using two SpS values: a first value  
263 of  $1482 \text{ m.s}^{-1}$  corresponding to the SpS recorded in pure water at a temperature of  $20 \text{ }^{\circ}\text{C}$ , and  
264 a second value of  $1509 \text{ m.s}^{-1}$  corresponding to a SpS at  $30 \text{ }^{\circ}\text{C}$  (Del Grosso and Mader, 1972).  
265 These values cover the temperature variations observed in our site during the experiment  
266 (Table 1). Hereafter, we refer to SpS values using their equivalent temperature ( $20 \text{ }^{\circ}\text{C}$  &  $30$   
267  $^{\circ}\text{C}$ ). We analyzed the effects of M using the matrices M1 and M2 that corresponded  
268 respectively to the hydrophone coordinates at the beginning and at the end of the experiment.  
269 PT parameters values were closely dependant on the user and on his experience of system  
270 operation. The influence of PT values was tested by using two independent sets of parameters  
271 defined by two persons using the same field data: 13 hours of survey of 17 tagged fish tracked  
272 on the 18 August 2009 throughout the site. The first set of PT values were defined by J. Bergé  
273 (PT-JB) and was based on an analysis of the influence of each parameter on the number of  
274 positioned points and the spatial consistency of these positions. The second set of PT values  
275 were defined by HTI<sup>®</sup> engineers (PT-HTI) using similar criteria but with greater acoustical

276 experience, and experience with the acoustic equipment and positioning software. Overall, we  
277 used a total of eight user defined combinations (2 SpS x 2 M x 2 PT, named C1 to C8 and  
278 detailed in Table 2) to infer the influence of user-defined variables.

279  
280 Among environmental variables (Table 3), the first group (configuration of hydrophones)  
281 included two variables. First, the viewing angle (C-VA, "C" for configuration) was defined as  
282 the angle needed, from the tag position, to view the polygon formed by the surrounding  
283 hydrophones (i.e. those located in a radius of 300 m, equal to the theoretical range of detection  
284 of hydrophone). When the tag was present inside the polygon, C-VA was equal to 360 °. The  
285 second variable was the number of hydrophones (C-NH) situated within a radius of 300 m.  
286 The second group of environmental variables (physical characteristics) described the physical  
287 environment at tag positions (detected or virtual). It included: the depth-averaged current  
288 velocity (P-CV, "P" for physical), the size of the dominant substrate in the water column  
289 relative to water depth (relative roughness, P-RR), the depth (P-Dp) and the water temperature  
290 (P-WT). P-CV and P-Dp were obtained from the hydraulic model, and P-WT was recorded by  
291 the NKE recorder (drags data) and by thermometers installed along the banks (temperatures  
292 were interpolated using spline functions for both sampling methods). The third group  
293 (indicators of reception conditions) included four variables potentially explaining positioning  
294 errors, and concerned detected positions only. The first variable was the maximal distance  
295 between the tag location and the hydrophones of the listening trio (I-MD, "I" for indicator).  
296 The second variable was the maximal angle of the triangle formed by the listening trio (I-  
297 MAT, in degrees) and illustrated the form of this triangle (flat triangle when I-MAT  
298 approaches 180 °). The third variable was the viewing angle needed, from the tag position, to  
299 view the triangle formed by listening trio (I-VA). The last variable was the amount of ambient  
300 noise, i.e. sounds produced naturally in the environment recorded by the listening trio

301 (Voegeli and Pincock, 1996). A Noise Ratio (I-NR, equivalent to the signal-to-noise ratio  
302 index used by Cote et al., 1998) was calculated for each hydrophone of the listening trio, by  
303 dividing (1) the highest amplitude of the received signal (echo) in samples recorded by the  
304 hydrophone, by (2) the average noise level recorded over 1 second prior to the signal  
305 reception. The minimum I-NR (maximum noise) of the listening trio was retained as  
306 explanatory variable.

307

## 308 *2.6. Data Analysis*

309

310 We analyzed the data in two steps. First, in a “within combination analysis”, we analyzed  
311 how environmental variables influenced the probability of detection and the positioning error  
312 within each combination (C1-C8). For this purpose, we produced plots of the average  
313 probability of detection and the average positioning error for ordinal categories of each  
314 environmental variable. We also produced smoothed maps of the probability of detection and  
315 the positioning error over the entire study site to check for spatial patterns related to the  
316 environment. The inter-correlation between environmental variables was checked using  
317 scatter plots and by computing Spearman rank correlation  $\rho$  for each pair of variables.

318

319 In a second step we performed a “between combination analysis”, i.e. we analyzed the  
320 average detection probability and the average positioning error associated with the eight  
321 combinations of user-defined variables (C1-C8), for drags and banks data. To better inform  
322 future users of the telemetry system, the effect of the 19 PT parameters was further detailed  
323 using a sensitivity analysis. Once the most accurate PT combination identified (PT-JB or PT-  
324 HTI), each parameter was modified in turn and was given two to four values within the usual  
325 range covered in practical applications. The set of values included the extreme values of the

326 usual range of the parameter, and the values chosen in PT-JB and PT-HTI. We quantified the  
327 changes in probability of detection and positioning error among the different parameter  
328 values.

329

### 330 **3. Results**

331

#### 332 *3.1. General functionality of the system*

333

334 Due to flow variability or scouring, four hydrophones did not work at all during the whole  
335 experiment; they included the first three hydrophones located in the upstream part of the study  
336 site (Fig. 1). Seven additional hydrophones did not work during the first drag, five during the  
337 second drag and two during bank measurements. For each data set, only functioning  
338 hydrophones were considered for calculating C-NH and C-VA. Six hydrophone positions  
339 could not be measured in September due to harsh hydraulic conditions, including the three  
340 hydrophones of the upstream part of the study site which never worked. For the three other  
341 hydrophones, we did not modify the coordinates of the hydrophones between matrices M1  
342 and M2. The comparison of M1 and M2 indicated that twelve hydrophones had moved: 10  
343 moved less than 6 m and two moved between 6 and 10 m. Concerning the positions estimated  
344 by the HTI<sup>®</sup> system (detected positions), approximately 40% of them presented duplicates  
345 which were not used for the analyses. In addition, 13.5 % of detected positions corresponded  
346 to positions extrapolated by the positioning software, i.e. that were derived using temporal  
347 extrapolations of reception signals at some hydrophones. These extrapolated positions can be  
348 identified and removed from the data base. However, we included these positions in our  
349 analyses because they were dependent on the choice of user-defined variables and were an

350 integral part of the positioning results. Finally, a total of 12,152 tag emissions (drag data) and  
351 1,140 tag emissions (banks data) were considered in our analyses.

352

### 353 *3.2. Environmental effects on detection probability within combinations*

354

355 A number of environmental variables influenced the probability of detection consistently  
356 within the eight combinations of user-defined variables (Fig. 3 and Fig. 4). Detection  
357 probability was mainly influenced by configuration variables. Detection probability increased  
358 with C-NH within all combinations, for banks and drags data: from < 10 % for C-NH < 6 to  
359 about 70 % for C-NH > 12 for drags data (Fig. 3a) and from 0 % for C-NH < 6 to about 30 %  
360 for C-NH > 14 for banks data (Fig. 4a). The detection probability also increased with C-VA  
361 from less than 5 % (drags and banks, Fig. 3b and 4b) to about 55 % for drags (Fig. 3b) and 20  
362 % for banks (Fig. 4b). Physical variables also influenced the probability of detection, since  
363 very high P-CV ( $> 1.44 \text{ m.s}^{-1}$ ) reduced the probability of detection from around 50 % to 20 %  
364 for drags (Fig. 3c), whereas low P-CV ( $< 0.52 \text{ m.s}^{-1}$ ) reduced the probability of detection from  
365 around 30 % to less than 10 % for banks (Fig. 4c). Low P-Dp ( $< 2.31 \text{ m}$ ) were also associated  
366 with reduced detection probabilities, for drags and banks (Fig. 3d and 4d). High P-RR values  
367 ( $> 2.8 \%$ , Fig. 3f) could reduce about twofold the probability of detection for drags, and to a  
368 lesser extent for banks (Fig. 4f). An intermediate temperature category was also associated  
369 with higher detection probabilities, but this temperature differed for drags (21.1 °C, Fig. 3e)  
370 and banks (17.44 °C, Fig. 4e). Banks data generally covered shallower and slower-flowing  
371 habitats (compare Fig. 3 and Fig. 4). They had a lower detection probability than drags on  
372 average, consistently with their low C-VA and high P-RR. However, detection probability  
373 was lower for banks data, even for comparable values of environmental variables.

374

375 Maps of detection probability showed similar spatial patterns among combinations (see Fig.  
376 5A for an example). The lowest detection probabilities were located where hydrophones did  
377 not function and thus where the configuration variables were not favorable. Furthermore,  
378 detection probability was lower along the river banks (Fig. 5A). Comparing Fig. 5A and 5B  
379 showed that the lowest probabilities of detection were located where the current velocity  
380 exceeded  $1.6 \text{ m.s}^{-1}$ . Scatter plots among environmental variables (see an example in  
381 Supplementary file S2) indicated that the influence of environmental variables could be  
382 complicated by a high positive correlation between C-NH and C-VA and a negative  
383 correlation between P-Dp and P-RR, for both drags and banks data. For drags data, C-NH was  
384 also negatively correlated with P-CV. For banks data, P-CV and P-Dp were positively related.  
385

### 386 *3.3. Environmental effects on positioning error within combinations*

387  
388 For detected tags, environmental variables had weaker relationships with positioning error  
389 than with detection probability (Fig. 6 and Fig. 7). Configuration variables were again the  
390 main driver of positioning error, which was reduced when C-NH was high ( $> 12$  for drags,  $>$   
391  $13$  for banks, Fig. 6a and 7a) and C-VA was high ( $> 156^\circ$  for drags and banks, Fig. 6b and  
392 Fig. 7b). However, these effects were not obvious for the two most accurate user-defined  
393 combinations for drags (C6 and C5). High roughness (P-RR) noticeably reduced the error for  
394 banks data (Fig. 7f) and high velocities (P-CV) increased the error of drags data for the worse  
395 combinations only (Fig. 6c). Finally, indicators of reception quality were consistently related  
396 to the error, that could be increased (by a factor less than two) when I-VA decreased (Fig. 6i  
397 and Fig. 7i) and when I-MD and I-MAT increased (Fig. 6g, 6h, 7g, 7h). I-NR had no obvious  
398 relationship with the error (Fig. 6j and Fig. 7j). Detected banks data had errors generally two  
399 times larger than drags data (Table 2). This was consistent with their C-VA and I-VA being

400 two times lower and their P-RR being ten times larger (see the Supplementary file S3). Note  
401 that I-NR of detected tags were two times lower for banks, i.e. though noise did not explain  
402 error variations within drags and banks data, it could partly explain differences between the  
403 two data sets.

404  
405 Maps of positioning errors of detected tags showed similar spatial patterns among  
406 combinations (see Fig. 8 for an example) and reflected that the environment affected  
407 positioning errors less than detection probability. The positioning errors were higher along  
408 river banks, and tended to be higher in areas where hydrophones did not function properly.  
409 Scatter plots among environmental variables (see an example in Supplementary file S2)  
410 indicated that their influence on positioning errors could be complicated by the same inter-  
411 correlations as those described for the probability of detection. In addition, they indicated  
412 strong correlations among the indicators of reception conditions (except I-NR) and the  
413 configuration variables for banks data.

414  
415 *3.4. Differences in detection probability and positioning error between combinations*

416  
417 The average probability of detection varied among user-defined combinations between 34.6  
418 % (combination C3) and 47.2 % (C5) for drags data (Table 2) and between 8.3 % (C3) and  
419 17.7 % (C5) for banks data (Table 2). It was higher when PT was PT-HTI and M was M2 (for  
420 drags and banks). The average positioning error varied more strongly between combinations:  
421 between 3.6 m (C6) and 10.7 m (C3) for drags data (Table 2) and between 7.7 m (C7) and  
422 22.3 m (C4) for banks data (Table 2). It was primarily influenced by PT (i.e. it generally  
423 reduced two-fold when PT was PT-HTI), and secondarily reduced when M was M2 and SpS  
424 was 30 (for drags only). Environmental variables did not differ much between combinations,

425 for both drags and banks (see the Supplementary file S3), and the most accurate combinations  
426 (C6 and C5) did not select particular environmental characteristics.

427  
428 The sensitivity analysis detailing the effects of PT parameters showed that the probability  
429 of detection was very sensitive (i.e. could be modified by about 40%) to a few software  
430 parameters influencing echo tracking (i.e. minimum and maximum number of echoes required  
431 for a series of echoes from one hydrophone, maximum gaps allowed in this series and  
432 maximum distance allowed between two echoes, Supplementary file S1). The average  
433 positioning error was mostly influenced (with modifications of about 10 m) by an  
434 interpolation parameter (number of echoes used to smooth positions, Supplementary file S1).  
435 Different values of these parameters potentially explained differences observed between the  
436 PT-HTI and PT-JB settings.

437

#### 438 **4. Discussion**

439

440 Our assessment test of the HTI<sup>®</sup> system in heterogeneous environmental conditions showed  
441 that the effects of intrinsic user-defined variables and environmental variables were largely  
442 independent. Environmental variables were the main variables affecting detection probability,  
443 principally the configuration of hydrophones around tags and secondarily relative roughness  
444 and velocity. For detected tags, user-defined variables (the post-treatment parameters and  
445 secondarily the knowledge of hydrophone positions) were the main determinants of  
446 positioning error. Configuration variables had only a secondary influence on the positioning  
447 error, especially along the banks.

448

449 In our study, the best user-defined combination provided an average detection probability  
450 of 44% in the channel (16% for banks) and an average positioning error of 3.6 m in the  
451 channel (9.5 m for banks). Our installation was less accurate than a few others made in more  
452 homogeneous physical conditions and/or with higher hydrophone densities: e.g., a probability  
453 of detection of 75 % in Niezgoda et al. (2002) obtained with a CDMA (Code Division  
454 Multiple Access, Lotek Map\_500<sup>TM</sup>) or positioning errors around 1 m in Semmens (2008)  
455 obtained with the same HTI system used in the present study. This was largely expected due  
456 to the nature of our experiment, whose originality was to test the system in harsh conditions  
457 for identifying the determinants of tag detection and positioning error and quantifying their  
458 effects.

459

460 Our study quantifies how configuration variables can dramatically influence detection  
461 probability, and to a lesser extent positioning errors, though the relative role of our two  
462 configuration variables was difficult to sort out due to inter-correlation. This effect of  
463 hydrophones configuration can partly explain differences in detection probability between  
464 previous studies. For example, the study of Niezgoda et al. (2002) obtained a high probability  
465 of detection with four hydrophones installed in a delta estuarine wetland with a density of one  
466 hydrophone for around 375 m<sup>2</sup>. In another study, Carol et al. (2007) reported a probability of  
467 detection of less than 10% with three hydrophones (Vemco radio-acoustic positioning system)  
468 installed in a Spanish reservoir with a density of one hydrophone for around 23,000 m<sup>2</sup> (one  
469 third of the triangle surface formed by the listening trio). In our study, we had on average one  
470 hydrophone for about 7,000 m<sup>2</sup>, and correspondingly intermediate detection probabilities.  
471 Other parameters such as transmitter power and frequency could also have contributed to  
472 differences among studies. For example, the lower frequency used by Niezgoda et al. (2002),  
473 i.e. 76 kHz, can also explain their higher detection probability.

474

475 The effect of hydrophone configuration on positioning error in our experiment was  
476 secondary compared to its effect on detection probability. Consistently, Carol et al. (2007)  
477 reported positioning errors of less than 1 m within the hydrophones array despite their low  
478 detection probability. Nevertheless, the influence of configuration (and in particular viewing  
479 angles) on positioning errors is consistent with previous results that reported higher errors  
480 outside the arrays of hydrophones (Juell and Westerberg, 1993; Kell et al., 1994; Ehrenberg  
481 and Steig, 2002; Niezgodá et al., 2002; Espinoza et al., 2011). In our study, both viewing  
482 angles and hydrophone densities were often low, largely explaining that our positioning errors  
483 could be higher than those obtained in some previous studies (e.g. Carol et al., 2007,  
484 Semmens, 2008).

485

486 The study of the effect of physical conditions at tag emissions is original to this study, and  
487 generally revealed weak effects on the probability of detection and the positioning error.  
488 However there was a negative influence of high relative roughness conditions. Higher  
489 velocities were associated with lower probabilities of detection for drags data, but this could  
490 be due to the negative correlation between velocity and the density of hydrophones (i.e.  
491 hydrophones did not work in high velocity areas). Similarly, higher detection probability in  
492 fast-flowing and deep conditions for banks data likely reflected a confounding effect: among  
493 points of the banks data, those with higher velocity and depth (the two variables being  
494 correlated) were closer to the main channel and were better detected. Similar confounding  
495 effects along the banks were reported by Melnychuk and Christensen (2009). Concerning the  
496 temperature, a weak effect of thermal conditions on detection probability was highlighted but  
497 was also likely confounded with spatial patterns. Indeed, the intermediate temperature

498 category associated with high detection probability was different for drags and banks, and was  
499 situated in the middle of the reach for both data sets.

500

501 Therefore, it is very likely that physical variables affect the probability of detection and the  
502 positioning error only through indirect mechanisms, as in fast-flowing zones where high  
503 velocities may damage hydrophones or their connections. The clearer effect of the physical  
504 environment is that a lower probability of detection was observed along banks, as expected  
505 and reported in previous studies. This effect probably results from weak configurations and  
506 high levels of sound reflection in these shallow areas with high relative roughness (Cato and  
507 Bell, 1992; Juell and Westerberg, 1993; Trevorrow, 1998; Boswell et al., 2007), as also  
508 suggested by our indirect indicators of reception quality.

509

510 Experience for tuning PT parameter values had, overall less influence on the probability of  
511 detection than environmental factors in our study. However, our sensitivity analysis indicated  
512 that a particular attention should be given in future applications to the parameters influencing  
513 echo tracking, since these can alter the probability of detection. The lower positioning error  
514 obtained with the expert parameter settings was partly due to an interpolation parameter  
515 (number of echoes used to smooth tag position tracks) whose tuning also requires attention.  
516 These results suggest that a full understanding of the parameter calibration process is  
517 necessary to get the best capabilities from the system, especially when the possibilities of  
518 parameter values are numerous and closely dependent on the physical characteristics of the  
519 study site.

520

521 At the core of our study, the knowledge of the positions of hydrophones (matrix M) and  
522 speed of sound (SpS) had much weaker influence on the positioning error than PT parameters.

523 This is surprising when considering their predominant role emphasized in the literature (Juell  
524 and Westerberg, 1993; Kell et al., 1994; Cote et al., 1998; Wahlberg et al., 2001). Still, M and  
525 SpS could affect positioning errors by a meter or more, and they would probably have played  
526 a more important role in better configuration conditions. It is also possible that our two M  
527 matrices were both inaccurate on the experimental days, but the hydraulic conditions of the  
528 site prevented us from checking this aspect. Using the coordinates of the hydrophones  
529 measured at the end of the experiment improved our results, and this procedure is  
530 recommended for future experiments in fast-flowing rivers. Indeed, it is likely that the  
531 hydrophones rapidly moved after deployment and then stabilized on the bed.

532

533 The main practical lesson of our methodological study is that fixed acoustic telemetry  
534 systems can be used efficiently in fast-flowing rivers with high stresses and velocities, where  
535 they provided a reasonable detection probability and positioning error, despite a relatively low  
536 density of hydrophones installed within a 234,600 m<sup>2</sup> area. The probability of detection and  
537 the positioning error obtained here can be certainly improved with higher hydrophone  
538 densities and/or reduced study areas. However, it would be satisfactory for a number of  
539 ecological studies for which a higher quantity of accurate positions is not needed. As an  
540 example, for studies on the relationships between the physical habitat and the detailed  
541 movement of many fish individuals of several fish species in our reach, a fixed telemetry  
542 system is appropriate and a positioning error of 3-5 m is satisfactory considering the  
543 uncertainty of the hydraulic model. The main limit of fixed telemetry systems in large rivers  
544 seems to be the difficulty of deployment, illustrated by the length of weighted cables that were  
545 needed in the Rhone River (16 km) and the number of hydrophones that were temporarily  
546 disconnected (up to 11 out of 32), mostly due to scouring around blocks or accidents with  
547 trees in fast-flowing areas.

548

549       Because our results quantify the probability of detection and the positioning error for a  
550 variety of intrinsic and environmental combinations, we hope that they provide useful  
551 guidelines for optimizing future installations. Recommendations for improving detection and  
552 errors certainly depend on the objectives of the telemetry study (Kell et al., 1994). Studies for  
553 which detection probability is important, for example when tracking animals with frequent  
554 and large movements, should pay a particular attention to local hydrophone densities and  
555 viewing angles. If banks are of particular importance in such studies, our results can be used  
556 to quantify how the hydrophone density and angles should be increased near the banks to  
557 obtain a satisfactory probability of detection. For studies for which positioning error is more  
558 important (e.g. for some studies on species interaction), our results suggest paying particular  
559 attention to system parameter values. Evaluation tests of the system would be particularly  
560 useful in such conditions and can serve to optimize intrinsic parameter values. In all cases,  
561 high roughness zones should be better covered. Zones with extreme velocities or temperature  
562 fluctuations should not be problematic for the probability of detection and the positioning  
563 error, but should be avoided if a risk of damaging the hydrophones is identified. We  
564 recommend paying particular attention to the hydrophone mounting and installation method in  
565 such conditions and to choose an aerial deployment of cables when possible.

566

### 567       *Acknowledgement*

568

569       The authors thank the Water Agency Rhône Méditerranée & Corse, Electricity of France  
570 (EDF), the European Union / FEDER, the General Direction of Irstea and the Aquitaine  
571 region for their financial support, the Nuclear Power Plant of Bugey (EDF) for their  
572 collaboration, Eric McNeil, Samuel Johnston, Patrick Neilson, Dave Ouellette, Pascal Roger

573 and Raphael Mons for their help during material installation and software calibration. Special  
574 thanks to Yann Le Coarer for his help with tachometer measures and to Alizés plongée® for  
575 its involvement in the diving operation. Finally, we thank the anonymous reviewers, André St  
576 Hilaire and Lise Vaudor for their comments and assistance.

577

## 578 *References*

579

580 Baras, E., Lagardère, J.P., 1995. Fish telemetry in aquaculture: review and perspectives.

581 Aquacult. Int. 3, 77-102.

582

583 Boswell, K.M., Wilson, M.P., Wilson, C.A., 2007. Hydroacoustics as a tool for assessing fish

584 biomass and size distribution associated with discrete shallow water estuarine habitats in

585 Louisiana. Estuaries and Coasts 30, 607-617.

586

587 Capra, H., McNeil, E., Bouillon, M.C., Pella, H., Alfaro, C., 2011. Relevance of 2D hydraulic

588 model to address fish behaviour in large rivers. La Houille Blanche. In press.

589

590 Capra, H., Pella, H., Oriol, E., 2008. Records from the water temperature of the Rhône river in

591 the summer of 2008. Electricity of France - Cemagref Rep., 37 p.

592

593 Carol, J., Zamora, L., García-Berthou, E., 2007. Preliminary telemetry data on the movement

594 patterns and habitat use of European catfish (*Silurus glanis*) in a reservoir of the River

595 Ebro, Spain. Ecol. Freshwat. Fish 16, 450-456.

596

- 597 Cato, D.H., Bell, M.J., 1992. Ultrasonic ambient noise in Australian shallow waters at  
598 frequencies up to 200 kHz. DSTO Mat. Res. Lab., Tech. Rep. MRL-TR-91-23, February,  
599 25 p.  
600
- 601 Clements, S., Jepsen, D., Karnowski, M., Schreck, C.B., 2005. Optimization of an acoustic  
602 telemetry array for detecting transmitter-implanted fish. N. Am. J. Fish. Manage. 25, 429-  
603 436.  
604
- 605 Cooke, S.J., Bunt, C.M., Schreer, J.F., 2004. Understanding fish behavior, distribution, and  
606 survival in thermal effluents using fixed telemetry arrays: a case study of smallmouth bass  
607 in a discharge canal during winter. Environ. Manage. 33, 140-150.  
608
- 609 Cooke, S.J., Niezgodá, G.H., Hanson, K., Suski, C.D., Phelan, F.J.S., Tinline, R., Philipp,  
610 D.P., 2005. Use of CDMA acoustic telemetry to document 3-D positions of fish:  
611 Relevance to the design and monitoring of aquatic protected areas. Mar. Technol. Soc. J.  
612 39, 17-27.  
613
- 614 Cote, D., Scruton, D.A., Niezgodá, G.H., Mckinley, R.S., Rowsell, D.F., Lindstrom, R.T.,  
615 Ollerhead, L.M.N., Whitt, C.J., 1998. A coded acoustic telemetry system for high  
616 precision monitoring of fish location and movement: application to the study of nearshore  
617 nursery habitat of juvenile Atlantic cod (*Gadus morhua*). Mar. Technol. Soc. J. 32, 54-62.  
618
- 619 Craven, S.W., Peterson, J.T., Freeman, M.C., Kwak, T.J., Irwin, E., 2010. Modeling the  
620 relations between flow regime components, species traits, and spawning success of fishes  
621 in warmwater streams. Environ. Manage. 46, 181-194.

622

623 Del Grosso, V.A., Mader, C.W., 1972. Speed of sound in pure water. J. Acoust. Soc. Am. 52,  
624 1442-1446.

625

626 Ehrenberg, J.E., Steig, T.W., 2002. A method for estimating the "position accuracy" of  
627 acoustic fish tags. ICES J. Mar. Sci. 59, 140-149.

628

629 Ehrenberg, J.E., Steig, T.W., 2003. Improved techniques for studying the temporal and spatial  
630 behavior of fish in a fixed location. ICES J. Mar. Sci. 60, 700-706.

631

632 Espinoza, M., Farrugia, T.J., Webber, D.M., Smith, F., Lowe, C.G., 2011. Testing a new  
633 acoustic telemetry technique to quantify long-term, fine-scale movements of aquatic  
634 animals. Fish. Res. 108, 364-371.

635

636 Fritsch, F.N., Carlson, R.E., 1980. Monotone piecewise cubic interpolation. SIAM J. Numer.  
637 Anal. 17, 238-246.

638

639 Geeraerts, C., Ovidio, M., Verbiest, H., Buysse, D., Coeck, J., Belpaire, C., Philippart, J.C.,  
640 2007. Mobility of individual roach *Rutilus rutilus* (L.) in three weir-fragmented Belgian  
641 rivers. Hydrobiologia 582, 143-153.

642

643 Heupel, M.R., Semmens, J.M., Hobday, A.J., 2006. Automated acoustic tracking of aquatic  
644 animals: scales, design and deployment of listening station arrays. Mar. Freshwater Res.  
645 57, 1-13.

646

647 Juell, J.E., Westerberg, H., 1993. An ultrasonic telemetric system for automatic positioning of  
648 individual fish used to track Atlantic salmon (*Salmo salar L.*) in a sea cage. *Aquacult.*  
649 *Eng.* 12, 1-18.

650  
651 Kell, L.T., Russell, I.C., Challis, M.J., 1994. Development of a high resolution tracking  
652 system for monitoring the movement of migratory fish past obstructions. *Proc. of the IFM*  
653 *25th annual study course*, 269-288.

654  
655 Lucas, M.C., Batley, E., 1996. Seasonal movements and behaviour of adult barbel *Barbus*  
656 *barbus*, a riverine cyprinid fish: implications for river management. *J. Appl. Ecol.* 33,  
657 1345-1358.

658  
659 Lukšienė, D., Sandström, O., Lounasheimo, L., Andersson, J., 2000. The effects of thermal  
660 effluent exposure on the gametogenesis of female fish. *J. Fish Biol.* 56, 37-50.

661  
662 Lyons, J., Lucas, M.C., 2002. The combined use of acoustic tracking and echosounding to  
663 investigate the movement and distribution of common bream (*Abramis brama*) in the  
664 River Trent, England. *Hydrobiologia* 483, 265-273.

665  
666 Melnychuk, M.C., Christensen, V., 2009. Methods for estimating detection efficiency and  
667 tracking acoustic tags with mobile transect surveys. *J. Fish Biol.* 75, 1773-1794.

668  
669 Meyer, L., Hinrichs, D., 2000. Microhabitat preferences and movements of the weatherfish,  
670 *Misgurnus fossilis*, in a drainage channel. *Environ. Biol. Fish.* 58, 297-306.

671

- 672 Minns, C.K., Kelso, J.R.M., Randall, R.G., 1996. Detecting the response of fish to habitat  
673 alterations in freshwater ecosystems. *Can. J. Fish. Aquat. Sci.* 53, 403-414.  
674
- 675 Niezgodá, G.H., Benfield, M., Sisak, M., Anson, P., 2002. Tracking acoustic transmitters by  
676 code division multiple access (CDMA)-based telemetry. *Hydrobiologia* 483, 275-286.  
677
- 678 O'dor, R.K., Andrade, Y., Webber, D.M., Sauer, W.H.H., Roberts, M.J., Smale, M.J., Voegeli,  
679 F.M., 1998. Applications and performance of Radio-Acoustic Positioning and Telemetry  
680 (RAPT) systems. *Hydrobiologia* 372, 1-8.  
681
- 682 Olden, J.D., Naiman, R.J., 2010. Incorporating thermal regimes into environmental flows  
683 assessments: modifying dam operations to restore freshwater ecosystem integrity.  
684 *Freshwater Biol.* 55, 86-107.  
685
- 686 Olivier, J.M., Carrel, G., Lamouroux, N., Dole-Olivier, M.J., Malard, F., Bravard, J.P.,  
687 Amoros, C., 2009. The Rhône River Basin. In: Tockner, K., Robinson, C.T., Uehlinger, U.  
688 (Eds.), *Rivers of Europe*. Academic Press, London, pp. 247-295  
689
- 690 Ovidio, M., Baras, E., Goffaux, D., Birtles, C., Philippart, J.C., 1998. Environmental  
691 unpredictability rules the autumn migration of brown trout (*Salmo trutta L.*) in the Belgian  
692 Ardennes. *Hydrobiologia* 372, 263-274.  
693
- 694 Ovidio, M., Capra, H., Philippart, J.C., 2007. Field protocol for assessing small obstacles to  
695 migration of brown trout *Salmo trutta*, and European grayling *Thymallus thymallus*: a

- 696 contribution to the management of free movement in rivers. Fisheries Manag. Ecol. 14,  
697 41-50.
- 698
- 699 Ovidio, M., Capra, H., Philippart, J.C., 2008. Regulated discharge produces substantial  
700 demographic changes on four typical fish species of a small salmonid stream.  
701 Hydrobiologia 609, 59-70.
- 702
- 703 Ovidio, M., Philippart, J.C., 2008. Movement patterns and spawning activity of individual  
704 nase *Chondrostoma nasus* (L.) in flow-regulated and weir-fragmented rivers. J. Appl.  
705 Ichthyol. 24, 256-262.
- 706
- 707 Pella, H., Capra, H., Foulard, S., 2007. Développement d'un MNT du haut Rhône à partir de  
708 relevés bathymétriques réalisés avec un sondeur multi-faisceaux. Revue française de  
709 photogrammétrie et de télédétection 186, 81-86.
- 710
- 711 Poff, N.L., Zimmerman, J.K.H., 2010. Ecological responses to altered flow regimes: a  
712 literature review to inform the science and management of environmental flows.  
713 Freshwater Biol. 55, 194-205.
- 714
- 715 R Development Core Team. 2010. R: A language and environment for statistical computing.  
716 R Foundation for Statistical Computing, Vienna, Austria. ISBN 3-900051-07-0.
- 717
- 718 Roger, M.C., Capra, C., Roger, P., Le Goff, G., 2010. Hydrobiological monitoring of the  
719 Bugey site in 2009. Electricity of France - Cemagref Rep. 69 p.
- 720

- 721 Semmens, B.X., 2008. Acoustically derived fine-scale behaviors of juvenile Chinook salmon  
722 (*Oncorhynchus tshawytscha*) associated with intertidal benthic habitats in an estuary. Can.  
723 J. Fish. Aquat. Sci. 65, 2053-2062.
- 724
- 725 Simpfendorfer, C.A., Heupel, M.R., Hueter, R.E., 2002. Estimation of short-term centers of  
726 activity from an array of omnidirectional hydrophones and its use in studying animal  
727 movements. Can. J. Fish. Aquat. Sci. 59, 23-32.
- 728
- 729 Smith, G.W., Urquhart, G.G., MacIennan, D.N., Sarno, B., 1998. A comparison of theoretical  
730 estimates of the errors associated with ultrasonic tracking using a fixed hydrophone array  
731 and field measurements. Hydrobiologia 372, 9-17.
- 732
- 733 Takac, F., Walford, J., 2006. Leica system 1200 - High performance GNSS technology for  
734 RTK applications. Proc. Conf. of Institute of Navigation GNSS - 19th International  
735 Technical Meeting of the Satellite Division, 26-29 September 2006, Fort Worth, TX: p.  
736 217-225.
- 737
- 738 Trevorrow, M.V., 1998. Boundary scattering limitations to fish detection in shallow waters.  
739 Fish. Res. 35, 127-135.
- 740
- 741 Vehanen, T., Bjerke, P.L., Heggenes, J., Huusko, A., Maki-Petays, A., 2000. Effect of  
742 fluctuating flow and temperature on cover type selection and behaviour by juvenile brown  
743 trout in artificial flumes. J. Fish Biol. 56, 923-937.
- 744

745 Voegeli, F.A., Pincock, D.G., 1996. Overview of underwater acoustics as it applies to  
746 telemetry. In: Baras, E. and Philippart, J.C. (Eds.), Proceedings of the First Conference  
747 and Workshop on Fish Telemetry in Europe (no. 4-4-0095). Belgium: University of Liège,  
748 pp. 23-30.

749

750 Wahlberg, M., Mohl, B., Madsen, P.T., 2001. Estimating source position accuracy of a large-  
751 aperture hydrophone array for bioacoustics. *J. Acoust. Soc. Am.* 109, 397-406.

752

753 Zamora, L., Moreno-Amich, R., 2002. Quantifying the activity and movement of perch in a  
754 temperate lake by integrating acoustic telemetry and a geographic information system.  
755 *Hydrobiologia* 483, 209-218.

756

757

758

759

760

761

762

763

764

765

766

767

768

769

770 **Figure Captions**

771

772 **Fig. 1.** Location of the Bugey site on the Rhône River in France. Hydrophone positions and  
773 survey points.

774

775 **Fig. 2.** Concrete block of 300 kg and its hydrophone.

776

777 **Fig. 3.** Probability of detection of drags data as a function of six environmental variables, for  
778 the eight combinations of user-defined variables. We fixed the limits of environmental  
779 categories so that their sizes were balanced for all combinations, taking into account that some  
780 discrete values had a high frequency. The average class size across combinations and classes  
781 was 2429 (standard deviation = 1051). Note that the x-axis was log-transformed for the P-RR  
782 variable.

783

784 **Fig. 4.** Probability of detection of banks data as a function of six environmental variables, for  
785 the eight combinations of user-defined variables. We fixed the limits of environmental  
786 categories so that their sizes were balanced for all combinations, taking into account that some  
787 discrete values had a high frequency. The average class size across combinations and classes  
788 was 228 (standard deviation = 16). Note that the x-axis was log-transformed for the P-RR  
789 variable.

790

791 **Fig. 5.** Map of detection probability for the combination C6 associated with minimum  
792 positioning errors (A), and map of depth-averaged velocity for a discharge rate of  $500 \text{ m}^3 \cdot \text{s}^{-1}$   
793 (B). For readability, detection probabilities were averaged by regular categories of water  
794 depth (<1m; 1-2m; 2-3m; 3-4m; >4m) and by regular longitudinal sub-reaches (50 m long).

795 Values of velocity were averaged by cells of the hydraulic model. Triangles, squares and  
796 circles correspond to hydrophones positions identified in the matrix M2.

797

798 **Fig. 6.** Positioning error of drags data as a function of six environmental variables and four  
799 indicators of reception quality, for the eight combinations of user-defined variables. We fixed  
800 the limits of environmental categories so that their sizes were balanced for all combinations,  
801 taking into account that some discrete values had a high occurrence. The average class size  
802 across combinations and classes was 985 (standard deviation = 504). Note that the x-axis was  
803 log-transformed for the P-RR variable.

804

805 **Fig. 7.** Positioning error of banks data as a function of six environmental variables and four  
806 indicators of reception quality for the eight combinations of user-defined variables. We fixed  
807 the limits of environmental categories so that their sizes were balanced for all combinations,  
808 taking into account that some discrete values had a high frequency. The average class size  
809 across combinations and classes was 28 (standard deviation = 5). Note that the x-axis was log-  
810 transformed for the P-RR variable and that outliers (positioning error > 30 m) were indicated  
811 using arrows in each panel.

812

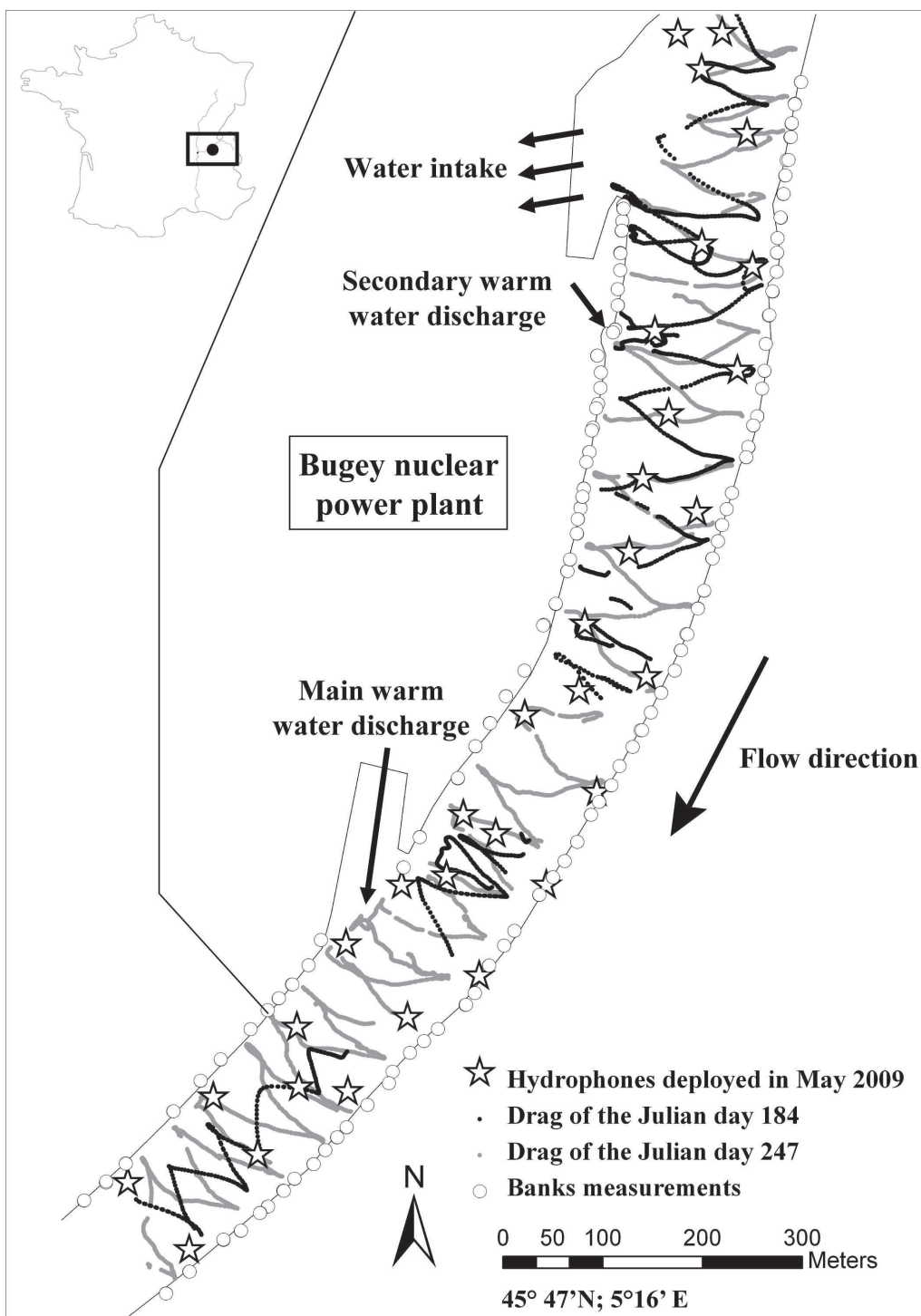
813 **Fig. 8.** Maps of positioning error for the combination C6. For readability, positioning errors  
814 were averaged by regular categories of water depth (<1m; 1-2m; 2-3m; 3-4m; >4m) and by  
815 regular longitudinal sub-reaches (50 m long). Triangles, squares and circles correspond to  
816 hydrophones positions identified in the matrix M2.

817

818

819

820 **Fig. 1**  
821



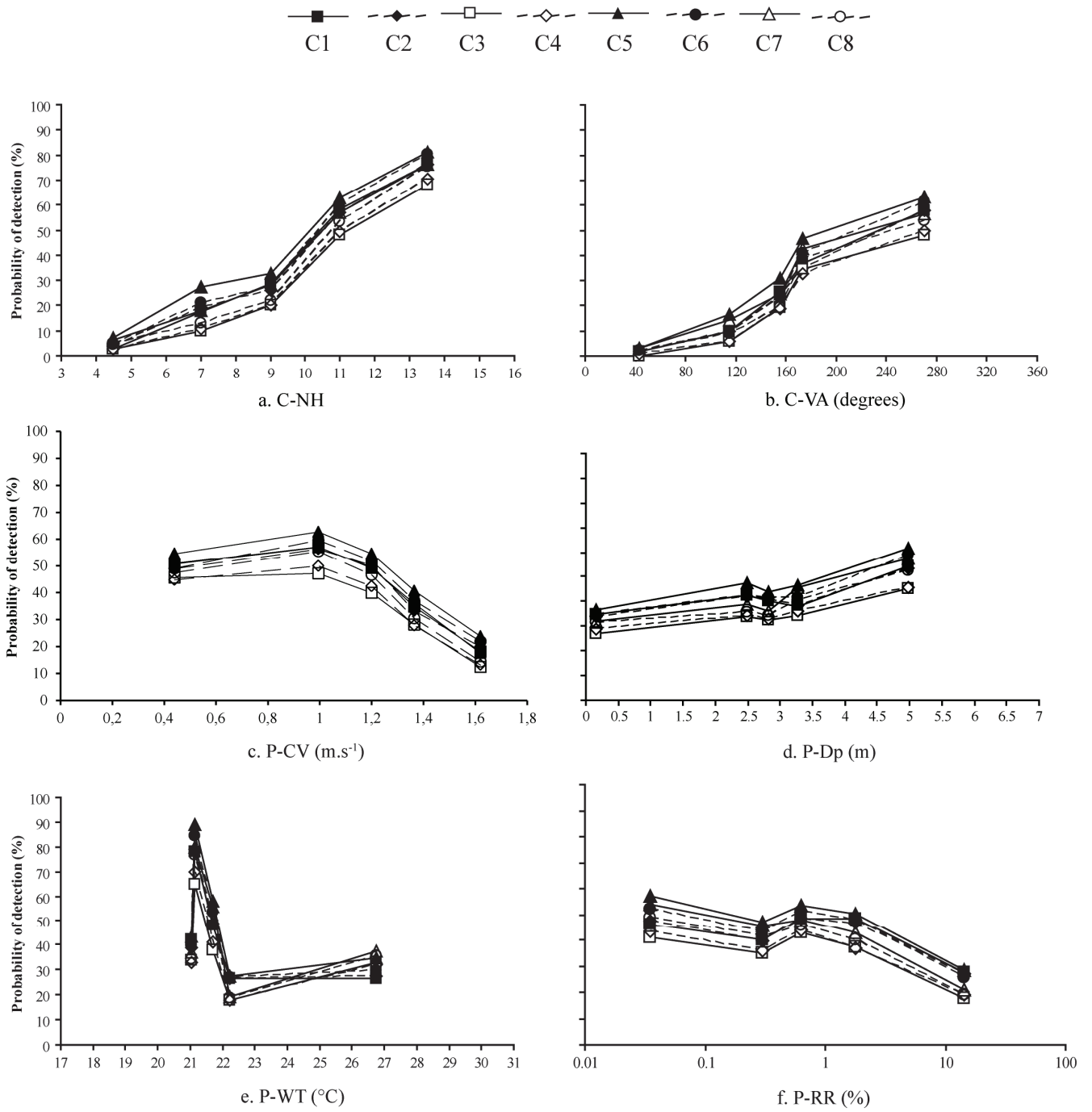
822  
823  
824

825 **Fig. 2**  
826



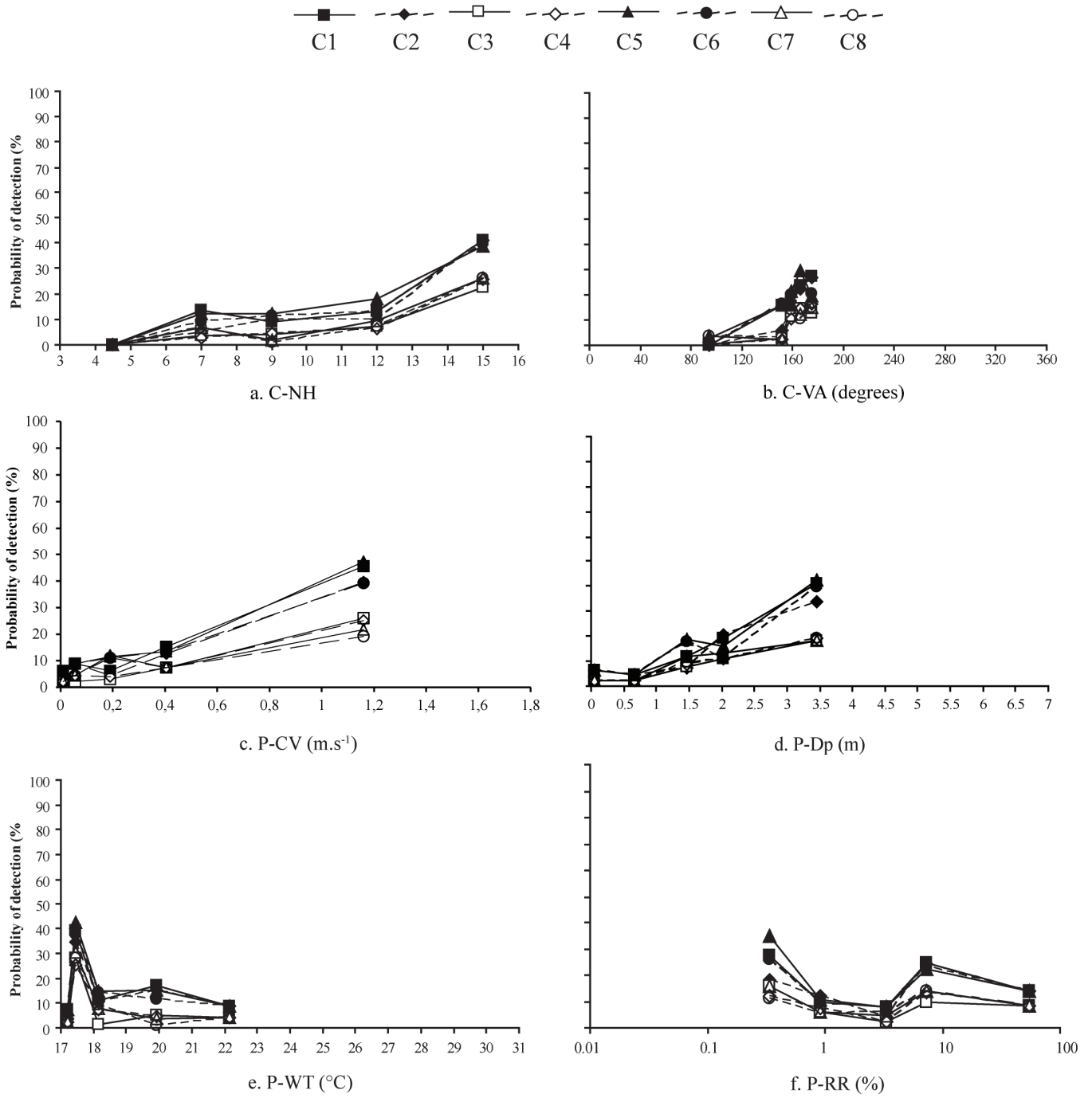
827  
828  
829

830 **Fig. 3**  
831



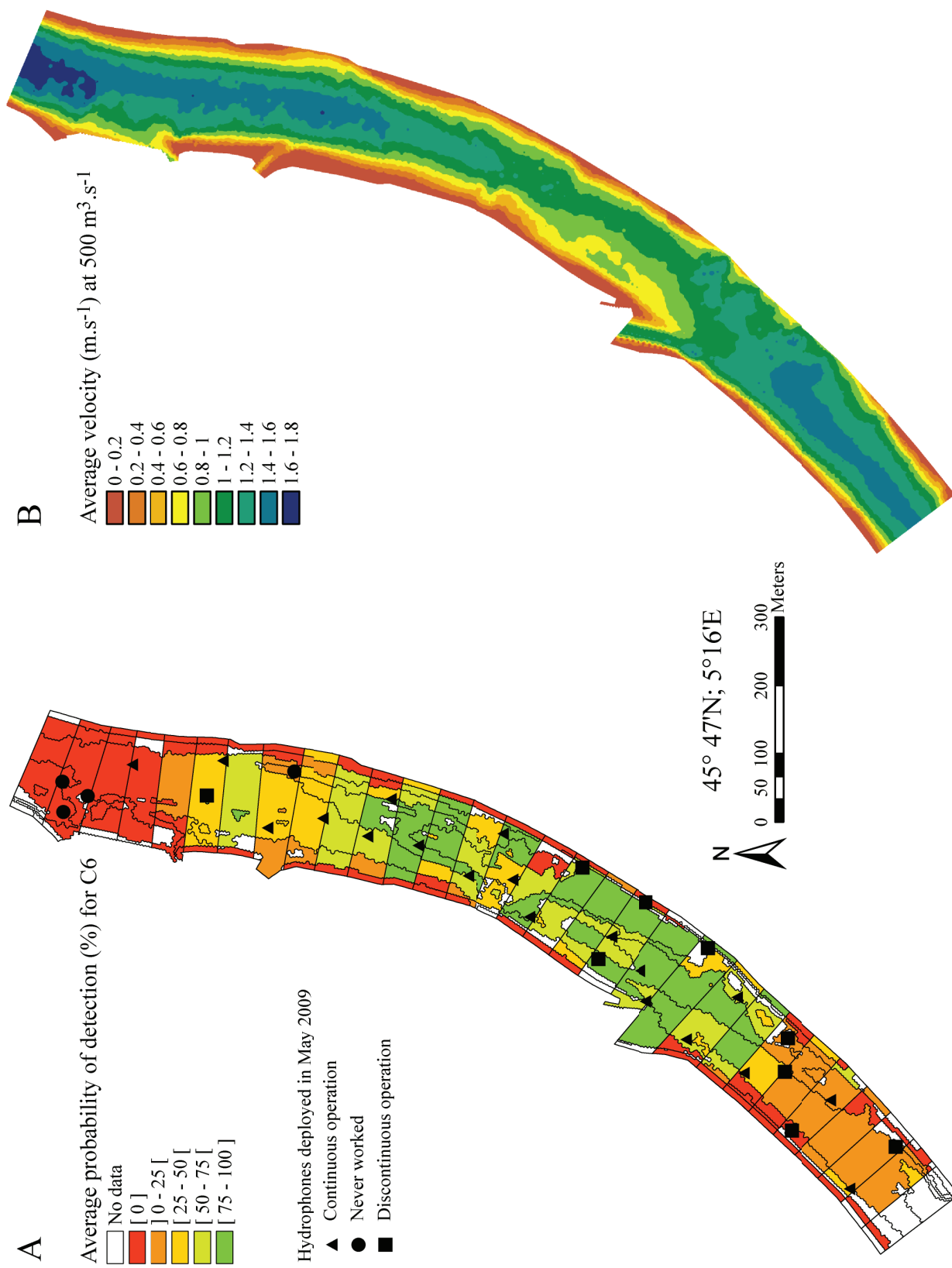
832  
833  
834

835 **Fig. 4**  
836



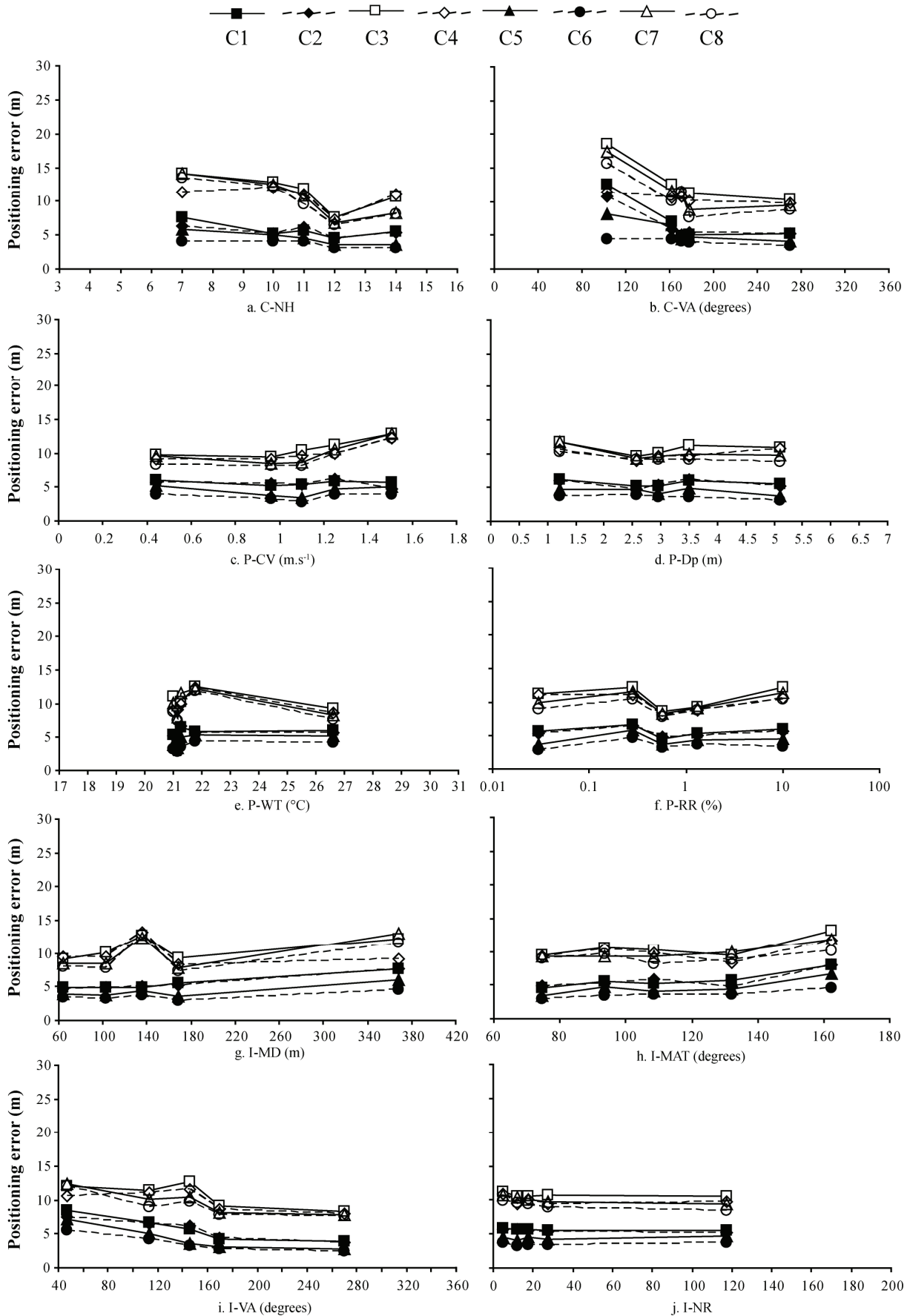
837  
838  
839

840 **Fig. 5**  
841



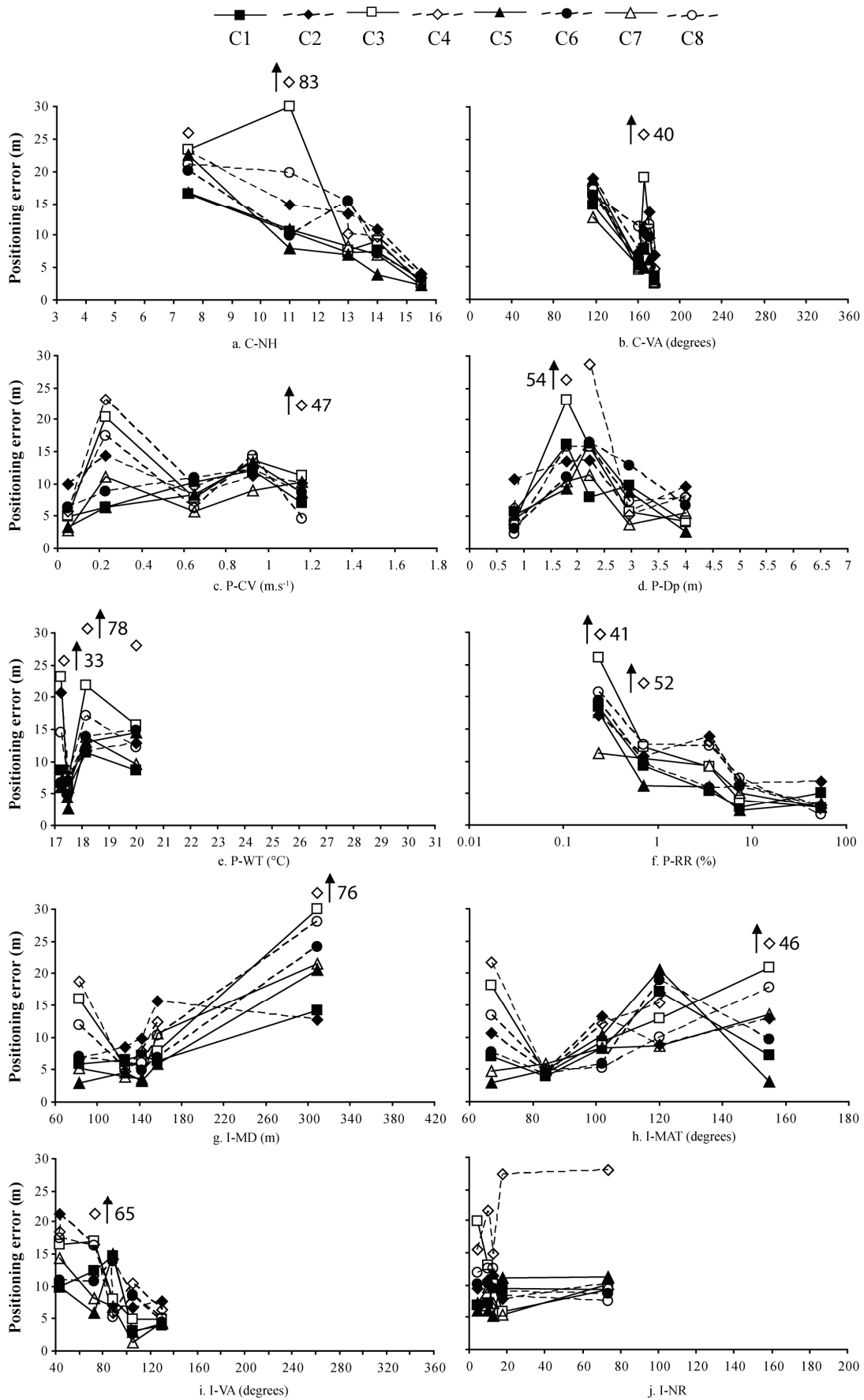
842  
843  
844

845 **Fig. 6**  
 846



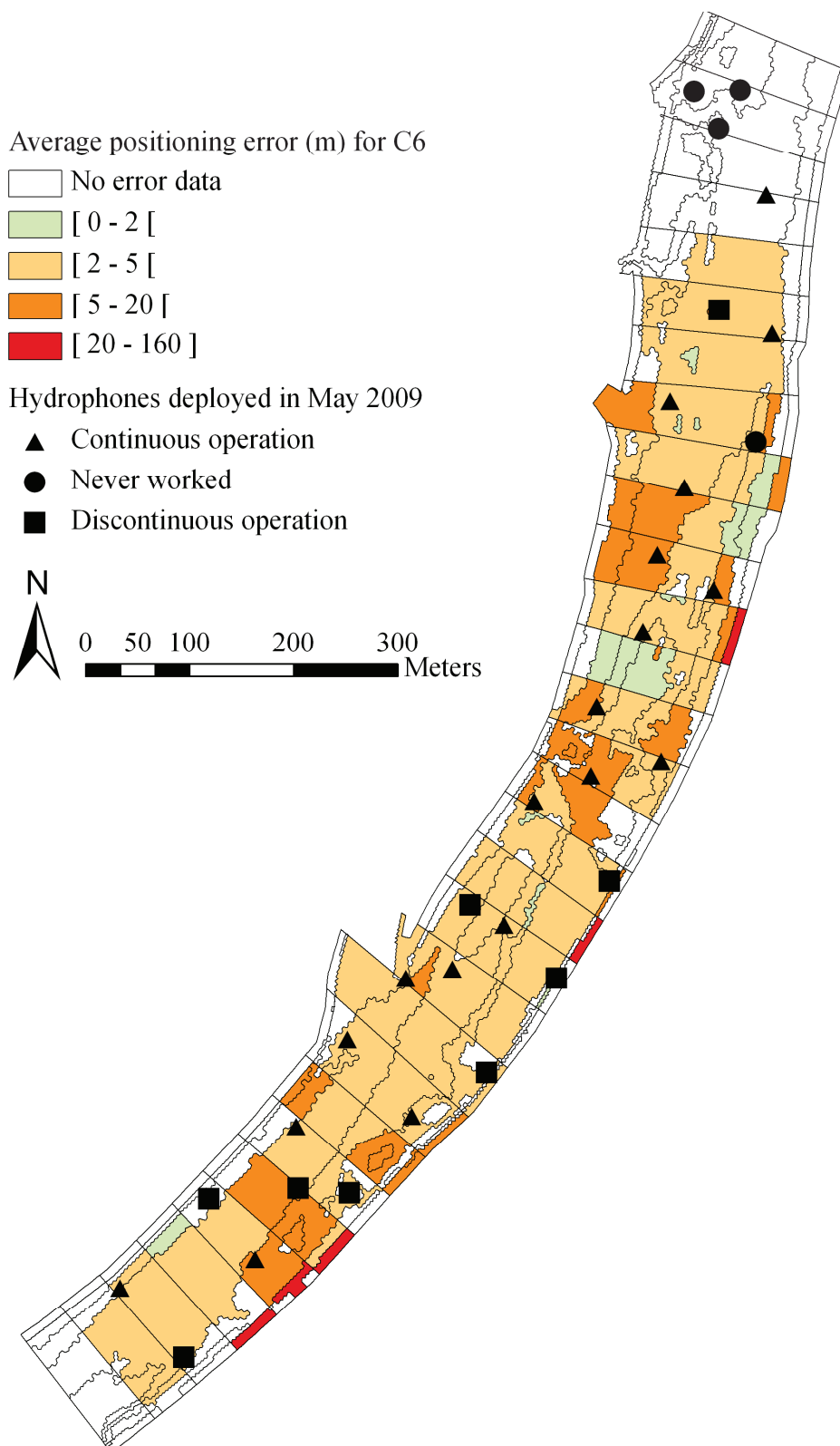
847

848 **Fig. 7**  
 849



850

851 **Fig. 8**  
852



853  
854  
855

856 **Table 1**

857 Characteristics of drags and banks data. Water temperatures are daily averages measured at  
858 fixed points situated upstream from the site and at power plant warm discharges.

859

Data set characteristics	Drags data		Banks data	
	July 3 <sup>rd</sup>	September 4 <sup>th</sup>	June 24 <sup>th</sup>	June 25 <sup>th</sup>
Recording time (min)	101.0	132.0	26.0	33.5
Daily discharge (m.s <sup>-1</sup> )	546.0	525.0	519.0	522.0
Water temperature (°C)				
Cold zone	22.1	21.1	17.3	18.4
Main power plant discharge	29.1	23.3	24.8	26.1
Secondary power plant discharge	31.5	30.1	26.0	27.4

860

861

Characteristics of the eight combinations defined for the treatment of drags and banks data: associated user-defined variables and statistics of probability of detection and positioning error. The mean positioning errors are given with their standard errors.

Combination	Methods Combinations							
characteristics	C1	C2	C3	C4	C5	C6	C7	C8
<i>User-defined variables</i>								
SpS (°C)	20	30	20	30	20	30	20	30
M	M1	M1	M1	M1	M2	M2	M2	M2
PT	HTI	HTI	JB	JB	HTI	HTI	JB	JB
<i>Accuracy statistics</i>								
Probability of Drag	41.9	41.6	34.6	35.5	47.2	43.9	42.1	38.9
detection (%) Bank	16.7	14.6	8.3	8.8	17.7	16.0	9.6	8.9
Mean Drag	5.7 ± 0.05	5.5 ± 0.08	10.7 ± 0.16	9.9 ± 0.16	4.5 ± 0.06	3.6 ± 0.05	10.1 ± 0.14	9.3 ± 0.14
positioning Bank	8.3 ± 0.62	10.7 ± 0.59	11.5 ± 1.24	22.3 ± 3.68	8.2 ± 0.70	9.5 ± 0.79	7.7 ± 0.80	10.5 ± 1.09
error (m)								

**Table 3**

Environmental variables: notations and definitions.

Environmental Variable	Symbol	Unit	Description
<i>Configuration variables</i>			
Viewing angle	C-VA	degrees	The angle needed, from the tag position, to view the polygon formed by the surrounding hydrophones
Density of hydrophones	C-NH		Number of hydrophones situated within a radius of 300 m around the tag location
<i>Physical characteristics</i>			
Current velocity	P-CV	m.s <sup>-1</sup>	Depth-averaged velocity at tag position
Relative roughness	P-RR	%	Substrate size divided by depth at tag position
Depth	P-Dp	m	Water depth at tag position
Water temperature	P-WT	°C	Water temperature at tag position
<i>Indicators of reception conditions</i>			
Maximal distance	I-MD	m	Maximal distance between the tag location and the hydrophones of the listening trio
Maximal angle of the triangle	I-MAT	degrees	Maximal angle of the triangle formed by the listening trio
Viewing angle	I-VA	degrees	The angle needed, from the tag position, to view the triangle formed by listening trio
Noise ratio	I-NR		Ratio of the highest amplitude of the received signal a hydrophone, by the average noise level recorded over 1 second prior to the signal reception

Probability of detection and positioning error of a hydro acoustic telemetry system in a fast-flowing river:  
intrinsic and environmental determinants

Julien Bergé, Hervé Capra, Hervé Pella, Tracey Steig, Michaël Ovidio, Elise Bultel, Nicolas Lamouroux.

#### Supplementary file S1

Description of the 19 Post-Treatment parameters (PT) used for the acoustic tag positioning. We indicated the usual range of each parameter in practical applications, as well as values corresponding to novice (PT-JB) and expert (PT-HTI) settings. Results of the sensitivity analysis report how the probability of detection and the positioning error varied when the value of each parameter was modified in turn, starting from the PT-HTI setting.  $\Delta$ HTI-JB is the average difference between the probability of detection (%) or positioning error (m) when the PT-HTI setting is used compared with the PT-JB setting; it has a positive value when the PT-HTI setting provides a higher probability of detection, and a negative value when the PT-HTI setting provides a lower positioning error.  $\Delta$ max is the maximum absolute difference observed among all pairs of values tested and represents the general sensitivity of the results to the parameter.

Software group	Parameter	ID	Unit	Parameter name	Parameter effect	Usual range												Sensitivity analysis					
						Drag						Bank											
						Min	Max	PT-JB	PT-HTI	$\Delta$ HTI-JB	$\Delta$ max	Error (m)	Detection (%)	$\Delta$ HTI-JB	$\Delta$ max	Detection (%)	Error (m)						
MarkTags	Tag Detection	1	-	Minimum	Minimum number of echoes that must be auto-tracked within each per Hydrophone	0	10	9	0	0	0	0	0	0	0	0	0	0	0				
	Data Selection	2	ms	Search Window	Time window (+/-) around the expected period in which an echo will be accepted as a tag pulse.	1/1	3/3	1.25/1.25	1/2	1	4	0	0	0	0	0	0	0	1				
	Subcode Verification	3	ms	Search Window around Subcode	Time window (+/-) around the expected subcode spacing used to verify an acceptable echo code and subcode.	1	5	1	5	-1	2	0	0	0	0	0	0	0	0				
	Subcode Selection	4	bins	Total Bins To Exceed	Number of bins around the theoretical subcode over which is an acceptable echo.	1	5	1	1	0	2	0	0	0	0	0	0	0	0				
	Echo Tracking	5	-	Minimum Acceptable Echoes	The minimum number of echoes acceptable for a series of echoes from one hydrophone.	1	10	8	4	7	17	0	1	5	9	-3	4						
		6	-	Maximum Acceptable Echo Gap	The maximum number of echo gap acceptable between a series of echoes from one hydrophone.	1	10	8	8	0	27	0	1	0	6	0	1						
		7	m.s <sup>-1</sup>	Maximum between echo Swim Speed	The distance over time that cannot be exceeded between echoes.	0	5	4	0.6	-4	5	0	0	1	1	0	0						



Table S1 (continued)

Software	Parameter	ID	Unit	Parameter name	Parameter effect	Usual range		Sensitivity analysis												
						Min	Max	Drag		Bank		Drag		Bank						
	Choosing	13	-	Geometry Type	Ignore: uses any hydrophone combination without regard to hydrophone location geometry. Require: only uses hydrophone combinations with user input minimum planar separation. The maximum time between position echoes over which interpolation will occur.	Ignore	Require	PT-JB	PT-HTI	Δ HTI- JB	Δ HTI- JB	Δ max	Error (m)	Detection (%)	Δ HTI- JB	Δ max	Error (m)	Δ HTI- JB	Δ max	
Hydrophones	Echo	14	s	Maximum Gap	The maximum time between position echoes over which interpolation will occur.	0	12	4	0	0	0	0	0	0	0	0	0	0	0	0
						0	6	5.5	0	0	0	0	0	0	0	0	0	0	0	0
Interpolation	Time Constant	16	-	Time Constant	The number of echoes used in smoothing the tag position tracks.	0	10	5	0	0	0	0	10	0	0	0	0	10	-1	3
						0	7	Normal	Normal	0	0	0	0	0	0	0	0	0	0	0
Solutions	Options	17	-	Transit (Normal or Advanced)	Normal transit does not attempt to use results when multiple valid solutions are calculated. This often occurs when the position is outside the array of hydrophones.	Normal	Advanced	Normal	Normal	0	0	0	0	0	0	5	0	0	3	



Probability of detection and positioning error of a hydro acoustic telemetry system  
in a fast-flowing river: intrinsic and environmental determinants

Julien Bergé, Hervé Capra, Hervé Pella, Tracey Steig, Michaël Ovidio, Elise Bultel, Nicolas  
Lamouroux.

Supplementary file S2

Figures S2.1 to S2.4 are pair-wise scatter plots showing the inter-correlation between pairs of environmental variables potentially explaining the detection probability and the positioning error of the telemetry system. Each figure concerns the probability of detection or the error, and is based on the drags or the banks data set. Each figure shows the frequency distribution of the environmental variables (diagonal), paired scatter plots (below the diagonal) and corresponding Spearman  $\rho$  values (above the diagonal). All Figures correspond to the results obtained for the user-defined parameters of the combination C6, see Table 2 in the full paper. Codes of the environmental variables are defined in Table 3 in the full paper.

Figure S2.1: Scatter plots corresponding to the environmental variables used to explain the probability of detection of drags data (Figure 3 in the full paper).

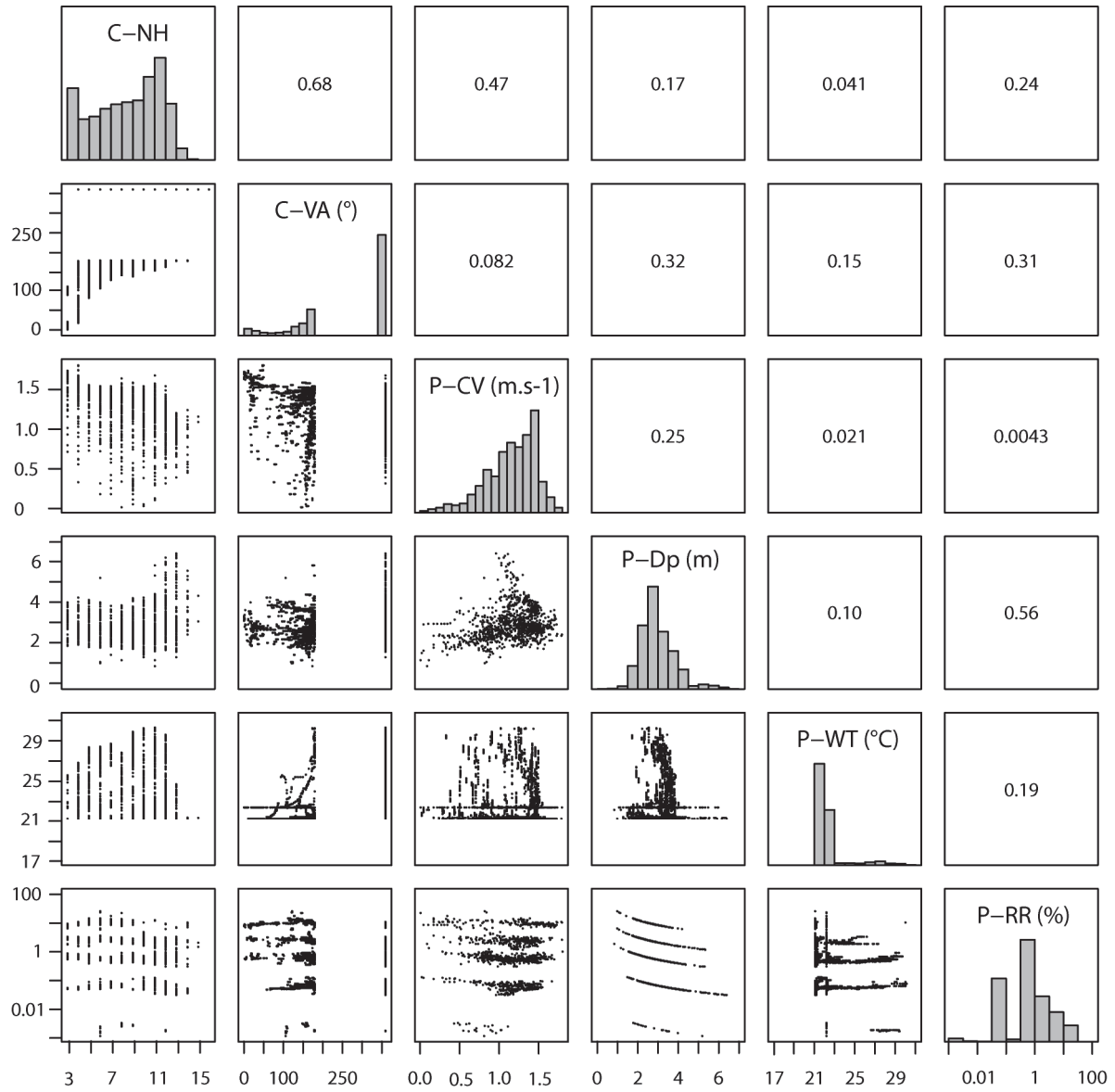


Figure S2.2: Scatter plots corresponding to the environmental variables used to explain the probability of detection of banks data (Figure 4 in the full paper).

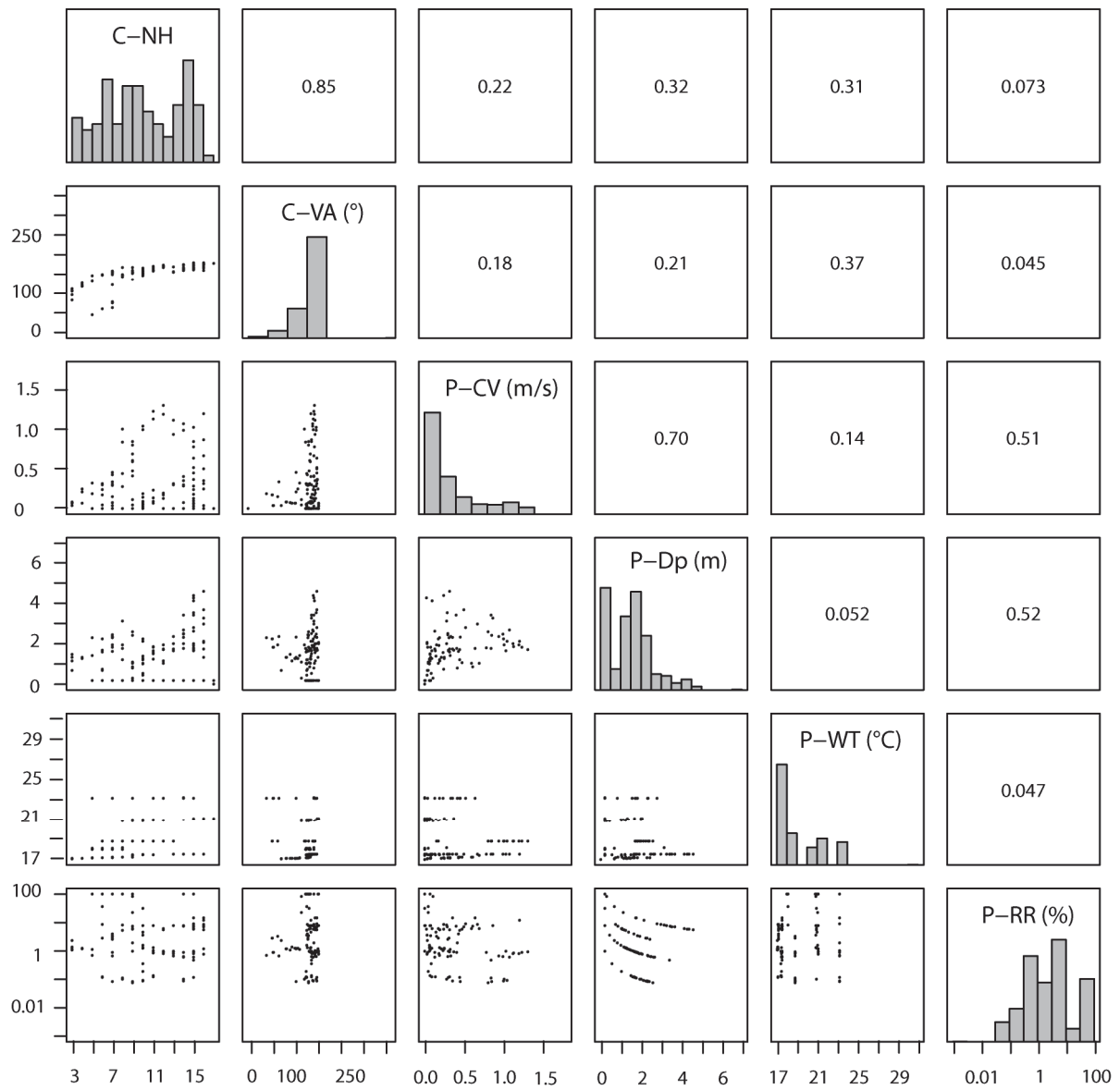
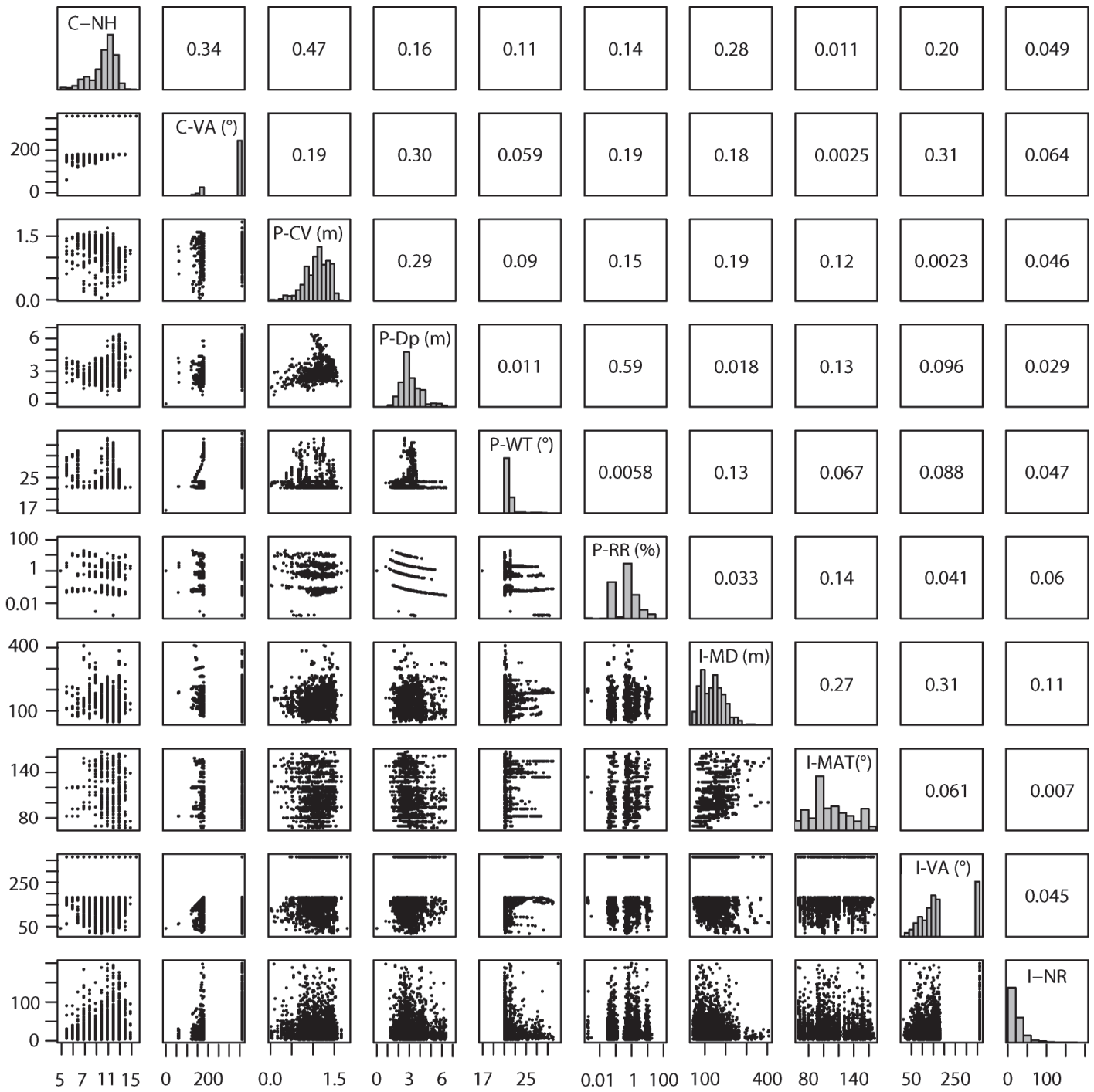


Figure S2.3: Scatter plots corresponding to the environmental variables used to explain the positioning error of drags data (Figure 6 in the full paper).





Probability of detection and positioning error of a hydro acoustic telemetry system in a fast-flowing river:  
 intrinsic and environmental determinants

Julien Bergé, Hervé Capra, Hervé Pella, Tracey Steig, Michaël Ovidio, Elise Bultel, Nicolas Lamouroux.

Supplementary file S3

Characteristics of the eight combinations of user-defined variables used to analyze drags and banks data: associated user-defined variables and average environmental characteristics of detected points ( $\pm$  standard errors). Codes of user-defined variables and environmental variables are from Table 3 in the full paper.

Combination characteristics	Combinations							
	C1	C2	C3	C4	C5	C6	C7	C8
<i>User-defined variables</i>								
SpS (°C)	20	30	20	30	20	30	20	30
M	M1	M1	M1	M1	M2	M2	M2	M2

PT	HTI	HTI	JB	HTI	JB	HTI	JB	HTI	JB
<i>Environmental variables-drags data</i>									
C-NH	11.0 ± 0.03	10.9 ± 0.03	11.1 ± 0.03	10.7 ± 0.03	11.1 ± 0.03	10.9 ± 0.03	10.8 ± 0.03	10.9 ± 0.03	11.0 ± 0.03
C-VA (°)	324.5 ± 1.08	325.9 ± 1.06	326.4 ± 1.14	327.7 ± 1.11	327.7 ± 1.11	324.5 ± 1.05	318.1 ± 1.15	324.5 ± 1.05	323.2 ± 1.13
P-CV (m.s <sup>-1</sup> )	1.1 ± 0.01	1.1 ± 0.01	1.1 ± 0.01	1.1 ± 0.01	1.1 ± 0.01	1.1 ± 0.01	1.1 ± 0.01	1.1 ± 0.01	1.1 ± 0.01
P-WT (°C)	21.6 ± 0.01	21.7 ± 0.02	21.8 ± 0.02	21.7 ± 0.02	21.8 ± 0.02	21.7 ± 0.02	21.8 ± 0.02	21.7 ± 0.02	21.8 ± 0.02
P-RR (%)	1.7 ± 0.04	1.7 ± 0.04	1.5 ± 0.04	1.6 ± 0.04	1.5 ± 0.04	1.6 ± 0.04	1.4 ± 0.04	1.6 ± 0.04	1.4 ± 0.04
P-Dp (m)	3.1 ± 0.01	3.1 ± 0.01	3.1 ± 0.01	3.1 ± 0.01	3.1 ± 0.01	3.1 ± 0.01	3.1 ± 0.01	3.1 ± 0.01	3.1 ± 0.01
I-MD (m)	143.6 ± 0.90	137.6 ± 0.77	136.1 ± 0.85	131.4 ± 0.79	131.4 ± 0.79	138.1 ± 0.76	148.5 ± 0.95	138.1 ± 0.76	131.4 ± 0.79
I-MAT (°)	110.0 ± 0.38	108.8 ± 0.37	116.6 ± 0.49	116.3 ± 0.47	116.3 ± 0.47	109.2 ± 0.35	115.4 ± 0.42	109.2 ± 0.35	117.7 ± 0.45
I-VA (°)	184.0 ± 1.49	188.5 ± 1.47	171.8 ± 1.58	177.5 ± 1.54	177.5 ± 1.54	184.2 ± 1.45	159.3 ± 1.42	184.2 ± 1.45	172.0 ± 1.47
I-NR	26.0 ± 0.51	26.2 ± 0.51	28.5 ± 0.57	28.3 ± 0.57	28.3 ± 0.57	26.6 ± 0.67	27.1 ± 0.58	26.3 ± 0.50	28.3 ± 0.65
<i>Environmental variables-banks data</i>									
C-NH	12.3 ± 0.22	12.8 ± 0.21	12.8 ± 0.28	12.1 ± 0.21	13.0 ± 0.25	12.3 ± 0.22	12.5 ± 0.27	12.3 ± 0.22	12.7 ± 0.28
C-VA (°)	165.7 ± 0.68	167.7 ± 0.61	165.9 ± 0.83	167.6 ± 0.77	167.6 ± 0.77	164.4 ± 0.63	161.5 ± 1.95	164.4 ± 0.63	159.2 ± 2.54
P-CV (m.s <sup>-1</sup> )	0.6 ± 0.03	0.6 ± 0.03	0.7 ± 0.04	0.6 ± 0.03	0.7 ± 0.04	0.6 ± 0.03	0.5 ± 0.04	0.6 ± 0.03	0.5 ± 0.04
P-WT (°C)	18.2 ± 0.09	18.2 ± 0.10	18.0 ± 0.11	18.2 ± 0.08	18.1 ± 0.11	18.2 ± 0.09	18.0 ± 0.11	18.2 ± 0.09	18.0 ± 0.12
P-RR (%)	14.6 ± 2.16	16.4 ± 2.44	14.1 ± 3.06	13.5 ± 2.05	13.9 ± 2.91	15.0 ± 2.25	12.8 ± 2.66	15.0 ± 2.25	13.9 ± 2.84

P-Dp (m)	2.3 ± 0.09	2.3 ± 0.10	2.2 ± 0.10	2.3 ± 0.12	2.2 ± 0.08	2.3 ± 0.09	2.3 ± 0.11	2.3 ± 0.12
I-MD (m)	169.0 ± 6.27	169.9 ± 6.29	159.3 ± 8.31	161.5 ± 8.19	157.9 ± 5.06	155.5 ± 5.39	144.2 ± 5.18	145.4 ± 5.70
I-MAT (°)	103.8 ± 2.13	110.4 ± 2.35	100.8 ± 2.84	111.4 ± 3.31	105.0 ± 2.22	105.3 ± 2.26	101.6 ± 2.83	106.3 ± 3.25
I-VA (°)	94.7 ± 2.25	96.8 ± 2.28	82.9 ± 2.99	92.7 ± 2.73	87.3 ± 1.98	91.1 ± 2.14	85.3 ± 2.42	87.3 ± 2.49
I-NR	15.4 ± 1.00	17.2 ± 1.38	15.9 ± 1.24	16.4 ± 1.21	14.7 ± 0.73	15.7 ± 0.84	15.9 ± 1.08	15.7 ± 1.24